

การศึกษาศักยภาพของส่วนผสมดินตะกอนกับซีเมนต์
เพื่ออุดรอยแตกในเกลือหิน



วิทยานิพนธ์นี้เป็นส่วนหนึ่งของการศึกษาตามหลักสูตรปริญญาวิศวกรรมศาสตรมหาบัณฑิต
สาขาวิชาเทคโนโลยีธรณี
มหาวิทยาลัยเทคโนโลยีสุรนารี
ปีการศึกษา 2556

**PERFORMANCE ASSESSMENT OF SLUDGE–
MIXED CEMENT GROUT IN
SALT FRACTURES**

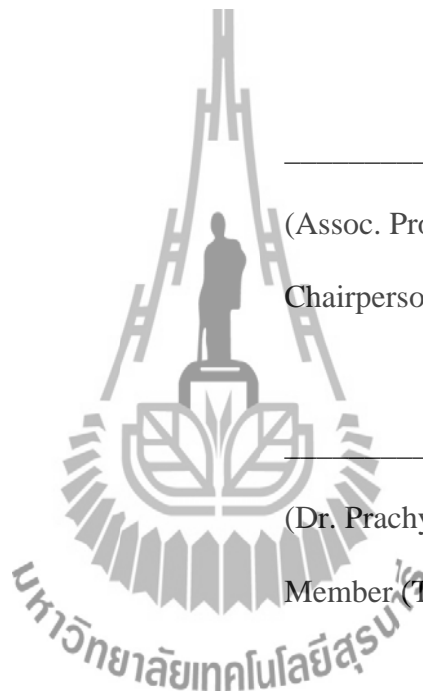


**A Thesis Submitted in Partial Fulfillment of the Requirements for the
Degree of Master of Engineering in Geotechnolgy
Suranaree University of Technology
Academic Year 2013**

**PERFORMANCE ASSESSMENT OF SLUDGE-MIXED
CEMENT GROUT IN SALT FRACTURES**

Suranaree University of Technology has approved this thesis submitted in partial fulfillment of the requirements for a Master's Degree.

Thesis Examining Committee



(Assoc. Prof. Kriangkrai Trisarn)

Chairperson

(Dr. Prachya Tepnarong)

Member (Thesis Advisor)

(Dr. Decho Phueakphum)

Member

(Prof. Dr. Sukit Limpijumngong)

Vice Rector for Academic Affairs
and Innovation.

(Assoc. Prof. Flt. Lt. Dr. Kontorn Chamniprasart)

Dean of Institute of Engineering

เผด็จ ดีท้าว : การศึกษาศักยภาพของส่วนผสมดินตะกอนกับซีเมนต์เพื่ออุดรอยแตกในเกลือหิน (PERFORMANCE ASSESSMENT OF SLUDGE-MIXED CEMENT GROUT IN SALT FRACTURES) อาจารย์ที่ปรึกษา : อาจารย์ ดร.ปรัชญา เทพณรงค์, 63 หน้า.

วัตถุประสงค์ของการศึกษานี้เพื่อประเมินศักยภาพของส่วนผสมดินตะกอนประปากับปูนซีเมนต์ในห้องปฏิบัติการสำหรับการอุดรอยแตกในเกลือหิน ซีเมนต์สำหรับอุดรอยแตกจัดเตรียมจากปูนซีเมนต์พอร์ตแลนด์ผสมด้วยดินตะกอนบำบัดน้ำประปาบางเขน น้ำเกลืออิ่มตัวและสารต้านคลอไรด์ ผลการทดลองที่ได้จะนำไปช่วยในการออกแบบซีเมนต์สำหรับอุดรอยแตกเพื่อลดการรั่วไหลที่จะมีโอกาสเกิดขึ้นจากการทิ้งกากของเสียจากอุตสาหกรรมในชั้นเกลือหินเหมือนใต้ดิน อุโมงค์ และท่อในเขตน้ำเค็ม แท่งตัวอย่างขนาดเส้นผ่านศูนย์กลาง 55 มม. เตรียมจากเกลือหินที่ได้จากการเจาะในเกลือชั้นกลางของหมวดหินมหาสารคาม ผลการทดสอบระบุว่าค่าของความหนืดของซีเมนต์อุดรอยแตกจะสูงขึ้นเมื่ออัตราส่วนผสมระหว่างดินตะกอนประปาและซีเมนต์ (S:C) เพิ่มขึ้น ค่ากำลังรับแรงกดสูงสุดที่อายุการบ่มตัว 28 วัน มีค่าเท่ากับ 9.58 ± 0.52 เมกะปาสคาล ค่าที่สูงที่สุดนี้ได้จากตัวอย่างที่ใช้อัตราส่วนผสม S:C = 5:10 ค่าเฉลี่ยกำลังรับดึงสูงสุดเท่ากับ 1.99 ± 0.14 เมกะปาสคาล ค่ากำลังยึดติดสูงสุดเท่า 7.9 เมกะปาสคาล การตรวจวัดค่าความซึมผ่านของซีเมนต์สำหรับอุดรอยแตกพบว่าเมื่อระยะเวลาของการบ่มตัวเพิ่มขึ้นค่าสัมประสิทธิ์การซึมผ่านจะลดลง ความเหมือนและความแตกต่างของประสิทธิภาพการอุดรอยแตกในเชิงกลศาสตร์และพลศาสตร์ของซีเมนต์ที่มีขายในเชิงพาณิชย์ได้นำมาเปรียบเทียบในการใช้อุดรอยแตกในเกลือหิน

สาขาวิชา เทคโนโลยีธรณี
ปีการศึกษา 2556

ลายมือชื่อนักศึกษา _____
ลายมือชื่ออาจารย์ที่ปรึกษา _____

PHADET DEETHOUW : PERFORMANCE ASSESSMENT OF SLUDGE-MIXED
CEMENT GROUT IN SALT FRACTURES. THESIS ADVISOR : PRACHYA
TEPNARONG, Ph.D., 63 PP.

FRACTURE / PERMEABILITY / GROUTING MATERIAL / SLUDGE / BRINE

The objective of this study is to experimentally assess the performance of sludge-mixed cement grouts for sealing fractures in rock salt. The cement grout is prepared from the commercial grade Portland cement mixed with Bang Khen water treatment sludge, brine and chloride resistant agent. The results are used to assist in the design of cement seal in rock fractures to minimize the brine circulation and potential leakage along the industrial waste repository in rock salt formation, underground mines, tunnels, and water pipes in saline regions. The salt specimens are prepared from the 54 mm diameter cores drilled from the Middle member of the Maha Sarakham formation. The results indicate that the viscosity of grout slurry tends to increase as the sludge-mixed cement (S:C) ratio increase. The compressive strength after 28 day curing times is 9.58 ± 0.52 MPa. The highest compressive strength is from ratio of S:C = 5:10. The average tensile strength is 1.99 ± 0.14 MPa. The highest bond strength is 7.49 MPa. When the curing time increases the intrinsic permeability of cement grouts decreases. Similarities and discrepancies of the grouting performance in terms of mechanical and hydraulic properties are compared to apply the commercial grade cement grouts in rock salt fractures.

School of Geotechnology

Student's Signature _____

Academic Year 2013

Advisor's Signature _____

ACKNOWLEDGEMENTS

The author wishes to acknowledge the support from the Suranaree University of Technology (SUT) who has provided funding for this research.

Grateful thanks and appreciation are given to Dr. Prachaya Tepnarong, thesis advisor, who lets the author work independently, but gave a critical review of this research. Many thanks are also extended to Assoc. Prof. Kriangkrai Trisarn and Assoc. Prof. Dr. Kittitep Fuenkajorn, who served on the thesis committee and commented on the manuscript.

Finally, I most gratefully acknowledge my parents and friends for all their supported throughout the period of this research.

Phadet Deethouw

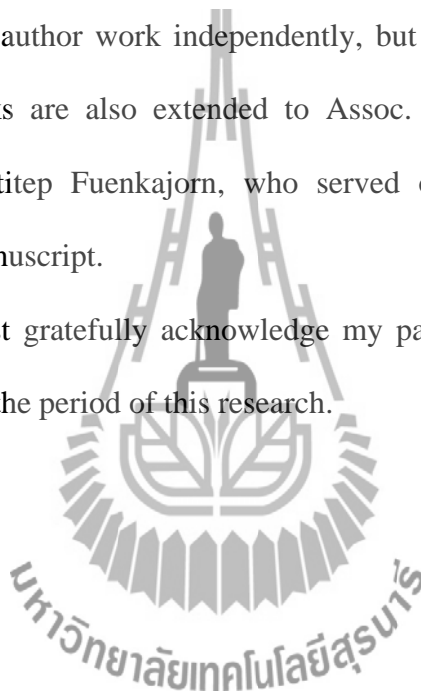


TABLE OF CONTENTS

	Page
ABSTRACT (THAI)	I
ABSTRACT (ENGLISH).....	II
ACKNOWLEDGEMENTS	III
TABLE OF CONTENTS.....	III
LIST OF TABLES	VI
LIST OF FIGURES	VII
LIST OF SYMBOLS AND ABBREVIATIONS.....	X
CHAPTER	
I INTRODUCTION.....	1
1.1 Background of problems and significance of the study.....	1
1.2 Research objectives	2
1.3 Research methodology	2
1.4 Scope and limitations of the study.....	5
1.5 Thesis contents.....	6
II LITERATURE REVIEW	7
2.1 Introduction.....	7
2.2 Rock salt formation in Thailand	7
2.3 Water treatment sludge from WMA	11
2.4 Flow ability of grouting slurry.....	13

TABLE OF CONTENTS (Continued)

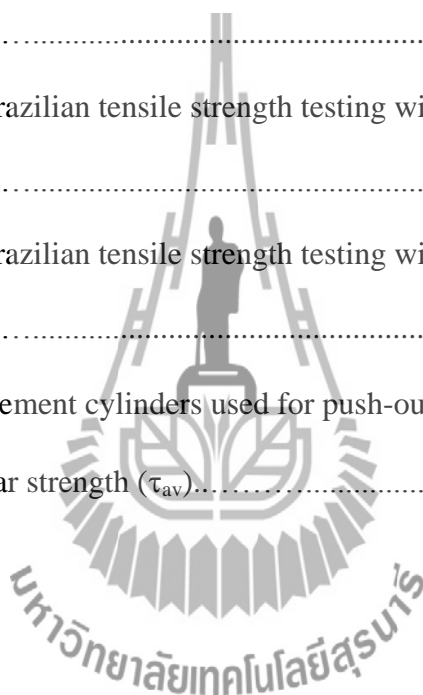
	Page
2.5 Permeability of grout	14
2.6 Strength of cured grout	17
III SAMPLE PREPARATION	21
3.1 Cement grout preparation	21
3.2 Rock salt specimen	22
IV LABORATORY TESTING	26
4.1 Introduction.....	26
4.2 Basic mechanical characterization of grouting materials	26
4.3 Push-out Resistance Tests.....	48
4.4 Permeability Testing of Grouting Materials	53
V DISCUSSIONS, CONCLUSIONS, AND RECOMMENDATIONS FOR FUTURE STUDIES	57
5.1 Discussions and conclusions	57
5.2 Recommendations for future studies	58
REFERENCES	59
BIOGRAPHY	63

LIST OF TABLES

Table	Page
3.1 Weight composition of sludge-mixed cement slurry.....	23
4.1 Viscosity and slurry density of cement slurry.....	28
4.2 Uniaxial compressive strength and elastic modulus of grouting material (S:C = 0:10).....	33
4.3 Uniaxial compressive strength and elastic modulus of grouting materials (S:C = 1:10).....	34
4.4 Uniaxial compressive strength and elastic modulus of grouting materials (S:C = 2:10).....	35
4.5 Uniaxial compressive strength and elastic modulus of grouting materials (S:C = 3:10).....	36
4.6 Uniaxial compressive strength and elastic modulus of grouting materials (S:C = 4:10).....	37
4.7 Uniaxial compressive strength and elastic modulus of grouting materials (S:C = 5:10).....	38
4.8 Results of the Brazilian tensile strength testing with Specimen of S:C = 0:10.....	42
4.9 Results of the Brazilian tensile strength testing with Specimen of S:C = 1:10.....	43

LIST OF TABLES (Continued)

Table	Page
4.10 Results of the Brazilian tensile strength testing with Specimen of S:C = 2:10.....	44
4.11 Results of the Brazilian tensile strength testing with Specimen of S:C = 3:10.....	45
4.12 Results of the Brazilian tensile strength testing with Specimen of S:C = 4:10.....	46
4.13 Results of the Brazilian tensile strength testing with Specimen of S:C = 5:10.....	47
4.14 Dimensions of cement cylinders used for push-out tests, the axial strength (σ_{ax}) and average shear strength (τ_{av}).....	50



LIST OF FIGURES

Figure	Page
1.1	Research methodology 3
2.1	Sakon Nakhon and Khorat Basins containing rock salt in the northeast of Thailand 8
2.2	Cross – section showing rock salt in Khorat basin 11
3.1	Grain size distribution of water treatment sludge 23
3.2	Sludge-mixed concrete specimens prepared for uniaxial compressive strength test having 54 mm in diameter with L/D ratio of 2.5 24
3.3	Sludge-mixed concrete specimens prepared for Brazilian tensile strength test having 54 mm in diameter with L/D ratio of 0.5..... 24
3.4	Salt specimens are placed into the inner borehole of sludge-mixed cement cylinder within the PVC mold for push-out tests..... 25
4.1	Measurement of the viscosity sludge – mixed cement slurry with Brookfield viscometer (Model RV) (ASTM D2196)..... 28
4.2	Uniaxial compressive strength test on 54 mm diameter spacemen of sludge mixed cement with L/D ratio 0.25. The specimen is loaded axially in compression machine..... 30
4.3	Specimen failed by uniaxial compressive strength test 31
4.4	Uniaxial compressive strength of sludge mixed cement as a function of curing time 32

LIST OF FIGURES (Continued)

Figure	Page
4.5	The elastic modulus of admixture concrete in curing time 32
4.6	Brazilian test on 54 mm diameter specimen of sludge-mixed cement. The specimen is loaded along the diameter in SBEL PLT-75 loading machine. (a) Pre-test specimen. 39
4.7	Post-tested specimen of Brazilian test 40
4.8	Brazilian tensile strength of sludge-mixed cement as a function of curing time 41
4.9	Schematic drawing of push-out resistance test setup..... 50
4.10	Push-out test setup 51
4.11	Applied shear stress vs. top axial rock salt core displacement for the push-out resistance test..... 51
4.12	Specimen after failure in the push-out test 52
4.13	Specimen after failure in the push-out test 52
4.14	Constant head flow test apparatus used for permeability testing of grouting materials..... 54
4.15	Conductivity of permeability of sludge-mixed cement as a function of time. 55
4.16	Intrinsic permeability of sludge-mixed cement as a function of time 56

SYMBOLS AND ABBREVIATIONS

K_f	=	Fracture conductivity
e	=	Hydraulic aperture
g	=	Acceleration due to gravity
ν	=	Kinematic viscosity
b	=	the spacing between fracture
k	=	the fracture permeability
e_0	=	the initial joint aperture
δe	=	the change of the joint aperture due to stresses acting on the joint
K_n	=	Normal stiffness of discontinuity
σ_z	=	Vertical stress applied to the discontinuity
σ_h	=	Horizontal stress applied to the discontinuity
β	=	Orientation of discontinuity
k_0	=	Initial fracture permeability
s	=	fracture spacing
σ_{ch}	=	Confining healing pressure in which the permeability is zero
σ_c	=	Effective confining stress
K	=	hydraulic conductivity
E	=	Elastic modulus
ϵ	=	Volumetric strains
σ_b	=	The indirect tensile strength

SYMBOLS AND ABBREVIATIONS (Continued)

P	=	the applied load when the sample fails
D and L	=	The diameter and thickness
Q	=	Flow rate
γ	=	Unit weight of water
μ	=	Dynamic viscosity
σ_c	=	Uniaxial compressive strength
σ_n	=	Normal stress
τ	=	Shear stress
τ_p	=	Peak shear strength
τ_r	=	Residual shear strength



CHAPTER I

INTRODUCTION

1.1 Background of problems and significance of the study

Sludge from Bang Khen Water Treatment Plant, Metropolitan Waterworks Authority of Thailand (MWA) has increased up to 247 tons/day. The sludge has been collected from the water treatment process. The sludge volume depends on the amount of sediment transported by rain water in raw water source. The sludge cake is usually taken to fill in abandoned land. After several years, Sludge has increased. It results in an excessively high deposition. Utilization of the sludge for other purposes is being considered in order to reduce the volumes of the sludge. (Wetchasat and Fuenkajorn, 2012)

One of solutions is to use the sludge to minimizing brine circulation in rock salt formation. Brine in rock salt is one of the key factors governing the mechanical stability of structures in salt formation. A common solution practice in the construction industry in to use bentonite-mixed with cement as a grouting material to reduce permeability in fracture salt. The lack of a true understanding of the permeability characteristic of the sludge-mixed cement in fractured rock make it difficult to predict the water flow in geological structure under the complex hydrogeological environment.

1.2 Research objectives

The objective of this study is to assess the performance of sludge-mixed cement grout for the sealing under saline environment. The sludge-mixed cement grout is prepared from the commercial grade Portland cement mixed with the water treatment sludge, brine and chloride resistant agent. Portland-pozzoland cement is chosen for its low brine demand, sulfate resistance and widely used in construction industry. The results are used to assist in the design of cement seal in salt fractures to minimize the brine circulation and potential leakage along the industrial waste repository in rock salt formation, underground mine, tunnels, and water pipes in saline regions.

1.3 Research methodology

The research methodology includes 1) literature review, 2) sample collection and preparation, 3) basic properties testing of grouting material, 4) permeability testing of grouting materials in PVC mold, 5) push-out resistance testing between grouting material and rock salt fracture, 6) analysis and comparisons, 7) discussions and conclusions, and 9) thesis writing and presentation (Figure 1.1).

1.3.1 Literature Review

Literature review is carried out to study the experimental researches on the water treatment sludge, grouting materials, and permeability of single fracture. The sources of information are from text books, journals, technical reports and conference papers. A summary of the literature review is given in the thesis.

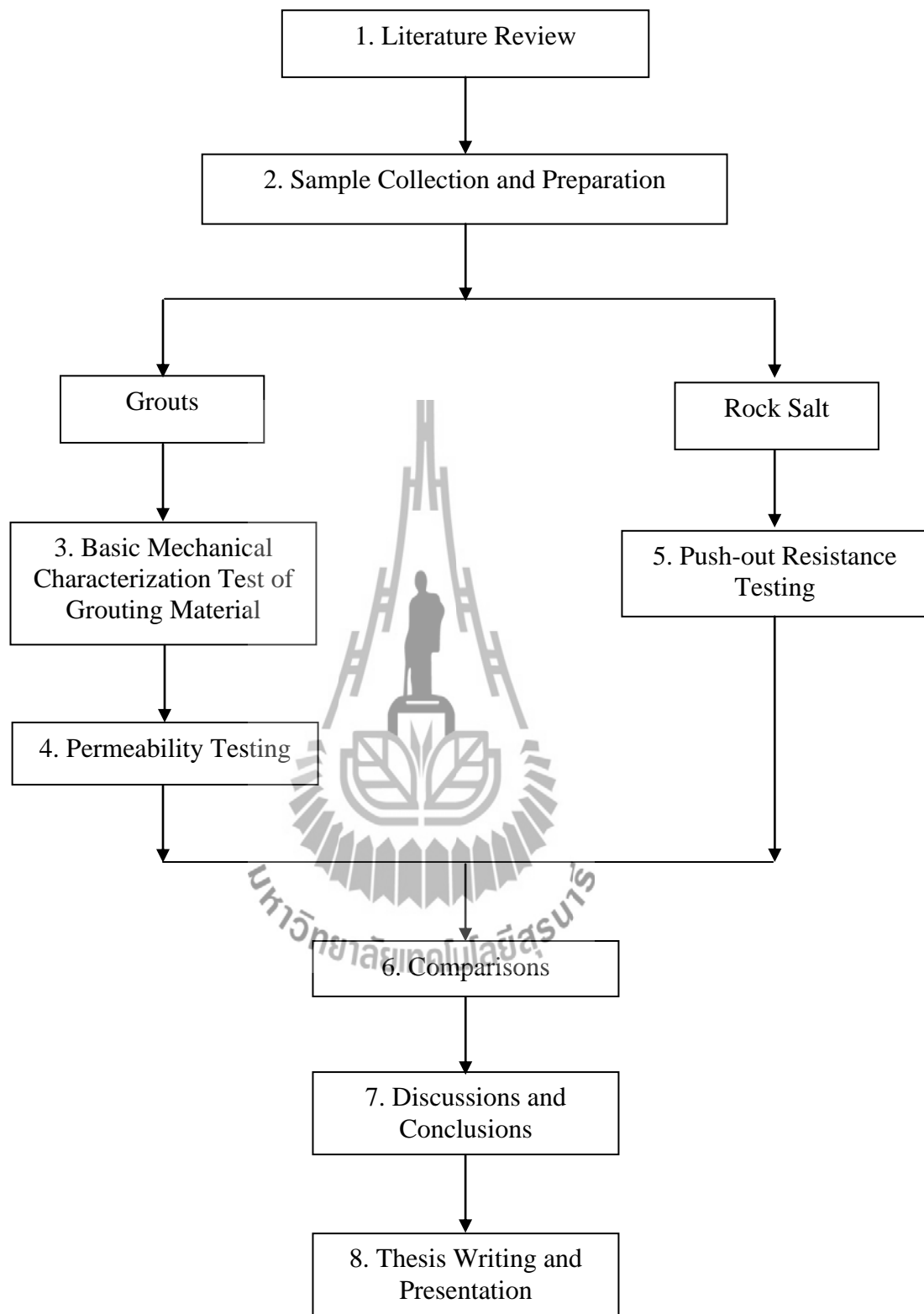


Figure 1.1 Research Methodology

1.3.2 Sample Collection and Preparation

The grouting materials used in this research are prepared from 1) the sludge with particle sizes less than 0.075 mm, 2) commercial grade Portland cement type V for mixing with the sludge and brine. 3) Mixing preparation is carried out in the laboratory at the Suranaree University of Technology. Rock salt specimens are prepared for the shear resistance test of rock joint by using push-out test.

1.3.3 Basic Mechanical Characterization Test of Grouting Materials

The basic mechanical properties of the mixtures are determined to select the appropriate proportions of sludge-to-cement ratios. The sludge-mixed cement ratios (S:C) 0:10, 1:10, 2:10, 3:10, 4:10 and 5:10 by weight are prepared with brine-sludge-mixed cement ratio of 1:1. Characterization testing provides the uniaxial compressive strength, elastic modulus, tensile strength, viscosity and slurry density of cement grout. The 54 mm diameter cylindrical sludge-mixed cement specimens are prepared by curing cement pastes in PVC molds for 7, 14, 21 and 28 days, respectively.

1.3.4 Permeability Testing

The permeability of grouting materials is determined in terms of the intrinsic permeability (k). The constant head flow test is conducted to measure the longitudinal permeability of the grout. The cylinder specimen is 4 inches in diameter and 4 inches long. The permeability of the test system is measured and recorded at 3, 7, 14, and 28 days of curing periods.

1.3.5 Push-out Shear Resistance Test

The objective of push-out shear resistance test use to determine the bond strength behavior between sludge-mixed cement and rock salt fracture. Push out

test determined the push out strength of rock salt core placed in the center of the sludge-mixed cement grout casted in PVC mold with a diameter of 100 mm and length of 100 mm. The sludge-mixed cement grouts casted in PVC mold are investigated after 7 days curing.

1.3.6 Comparisons

The experiment results are analysis to optimizing the sludge-mixed to cement ratio in terms of the mechanical and hydraulic properties. The results from data analysis are used to comparison with other researches.

1.3.7 Discussions and Conclusions

Discussions of the results are described to determine the reliability and accuracy of the measurements. Performance of the sludge-mixed cement grouting material are discussed based on the test results. Similarities and discrepancies of the grouting material in terms of the mechanical and hydraulic properties are discussed. The research results are concluded.

1.3.8 Thesis writing and presentation

All research activities, methods, and results are documented and complied in the thesis. The research or findings will be published in the conference proceedings or journals.

1.4 Scope and Limitations of the Study

The scope and limitations of the research include as follows.

1. This research emphasizes on studying the mechanical and hydraulic properties of water treatment sludge-mixed cement as a grouting material to reduce permeability in rock salt fracture.

2. Laboratory testing will be conducted on specimens from Maha Sarakam rock salt.
3. The permeability testing of sludge-mixed cement in PVC mold is performed by constant head flow tests with saturated brine.
4. Portland cement type V is used (ASTM C595).
5. The particle sizes of the sludge are less than 0.075 mm (sieve no. 200).
6. The sludge-to-cement (by dry weight) ratios of 1:10, 2:10, 3:10, 4:10, and 5:10 are primarily selected.
7. Mixing, curing and testing of the cement and mixtures follows, as much as practical, the ASTM and the API standards.
8. All tests are conducted under ambient temperature.

1.5 Thesis Contents

Chapter I states the objectives, rationale, and methodology of the research. **Chapter II** summarizes results of the literature review on sludge-mixed cement knowledge. **Chapter III** describes calibration procedure sample and mixture preparations. **Chapter IV** presents the results obtained from the laboratory testing. The experiments are divided into five tests, including (1) viscosity test, (2) uniaxial compressive strength test, (3) Brazilian tensile strength test, (4) the permeability test, (5) push-out shear resistance test. Conclusions and recommendations for future research needs are given in **Chapter V**.

CHAPTER II

LITERATURE REVIEW

2.1 Introduction

Topics relevant to this research are reviewed to improve an understanding of sludge-mixed cement. Study the experimental researches on the water treatment sludge, grouting materials, and permeability of single fracture. The sources of information are from text books, journals, technical reports and conference papers.

2.2 Rock Salt formation in Thailand

Rock salt formation in Thailand is located in the Khorat plateau as shown in Figure 2.1. The Khorat plateau covers 150,000 square kilometers, from 14° to 19° northern latitude and 101° to 106° eastern longitude. The northern and eastern edges of the plateau lie close to Laos and the southern one close to Cambodia (Utha-aroon, 1993).

Rock salt is separated into 2 basins: Sakon Nakhon Basin and Khorat Basin. The Sakon Nakhon Basin in the north has an area about 17,000 square kilometers. It covers the area of Nong Khai, Udon Thani, Sakon Nakhon, Nakhon Phanom, and Mukdahan provinces and extends to some part of Laos. The Khorat Basin is in the south, which has about 33,000 square kilometers. The basin covers the area of Nakhon Ratchasima, Chaiyaphum, Khon Kaen, Maha Sarakham, Roi Et, Kalasin, Yasothon, Ubon Ratchathani provinces and the north of Buriram, Surin, and Sisaket provinces (Suwanich, 1986).

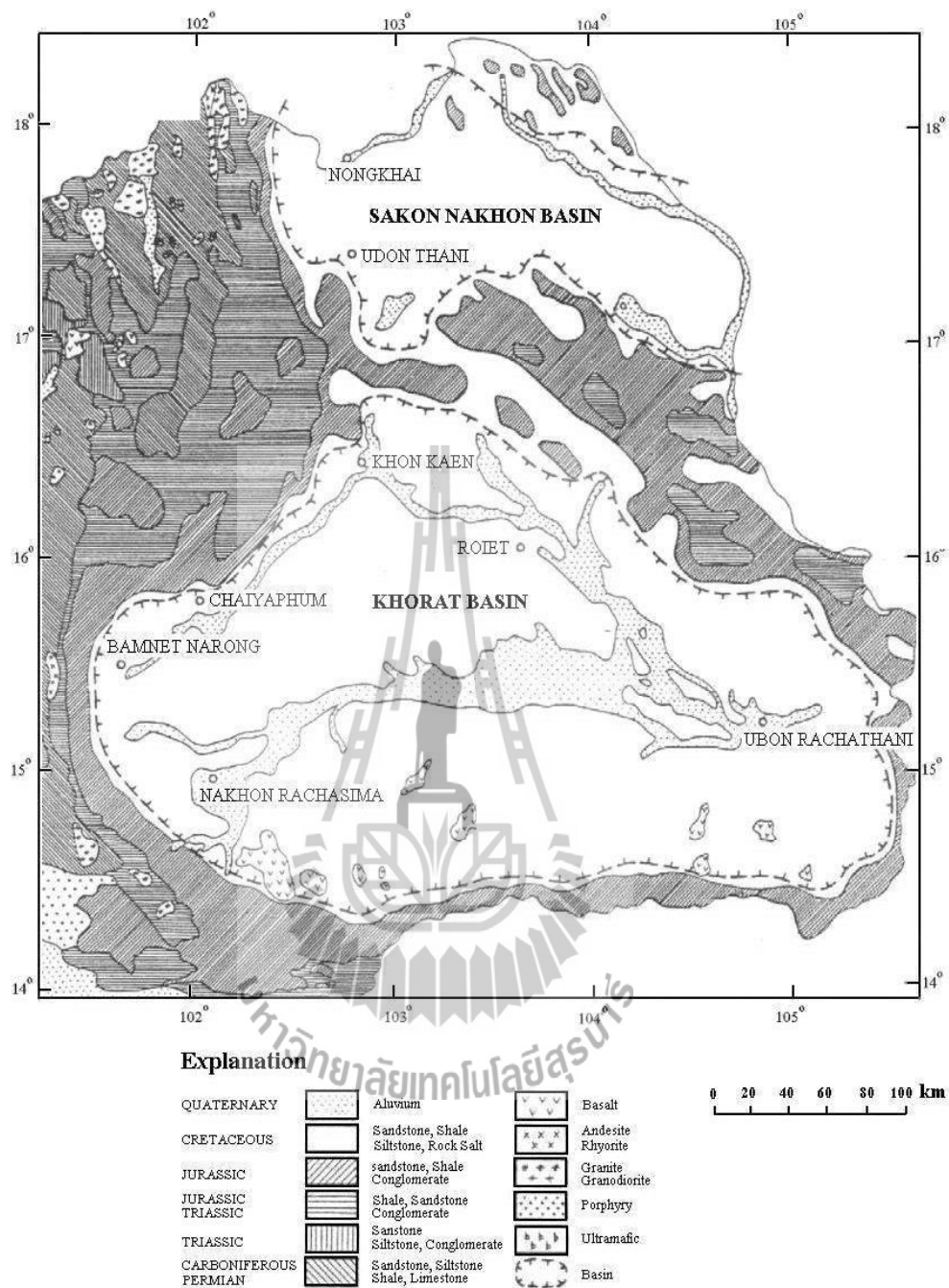


Figure 2.1 Sakon Nakhon and Khorat Basins containing rock salt in the northeast of Thailand (modified from Rattanajarurak, 1990 and Utha-aaron, 1993 adapted from Geological Map of Thailand, scale 1:2,500,000)

The Department of Mineral Resources had drilled 194 drilled holes between 1976 and 1977 for the exploration of potash (Japakasetr, 1985; Japakasetr and Workman, 1981; Sattayarak, 1983, 1985; Japakasetr, 1992; Japakasetr and Suwanich, 1982). Some holes were drilled through rock salt layers to the Khok Kruat Formation (Yumuang et al., 1986; Supajanya et al., 1992; Utha-aroon, 1993; Warren, 1999). The sequences of rock layers from the bottom of this formation up to the top of the Maha Sarakham Formation are as follows.

- 1) Red bed sandstone or dense greenish gray siltstone sometime intercalated with reddish-brown shale.
- 2) Basal anhydrite with white to gray color, dense, lies beneath the lower rock salt and lies on the underlying Khok Kruat Formation.
- 3) Lower rock salt, the thickest and cleanest rock salt layer, except in the lower part which contains organic substance. The thickness exceeds 400 meters in some areas and formed salt domes with the thickness up to 1,000 meters, with the average thickness of 134 meters.
- 4) Potash, 3 types were found; carnallite ($\text{KCl}\cdot\text{MgCl}_2\cdot 6\text{H}_2\text{O}$) with orange, red and pink color, sylvinite (KCl) rarely found, white and pale orange color, an alteration of carnallite around salt domes, and techydrate ($\text{CaCl}_2\cdot 2\text{MgCl}_2\cdot 12\text{H}_2\text{O}$) often found and mixed with carnallite, orange to yellow color caused by magnesium, the dissolved mineral occurred in place.
- 5) Rock salt, thin layers with average thickness of 3 meters, red, orange, brown, gray and clear white colors.
- 6) Lower clastic, clay and shale, relatively pale reddish-brown color and mixed with salt ore and carnallite ore.

7) Middle salt, argillaceous salt, pale brown to smoky color, thicker than the upper salt layer with average thickness of 70 meters, carnallite and sylvite may be found at the bottom part.

8) Middle clastic, clay and shale, relatively pale reddish brown color and intercalated with white gypsum.

9) Upper salt, dirty, mixed with carbon sediment, pale brown to smoky color or orange color when mixed with clay and 3 to 65 meters thick.

10) Upper anhydrite, thin layer and white to gray color.

11) Clay and claystone, reddish brown color, occurrence of siltstone and sandstone in some places, and

12) Upper sediment, brownish gray clay and soil in the upper part, and sandy soil and clay mixed with brown, pink and orange sandy soil in the lower part.

Cross-sections from seismic survey across the Khorat-Ubon and Udon-Sakon Nakhon Basins (Sattayarak and Polachan, 1990) reveal that rock salt can be categorized into 3 types according to their appearances namely, rock salt beds, rock salt fold and salt domes. The Maha Sarakham and Phu Tok Formations fold in harmony with the Khorat megasequence. A part of the cross section through the Khorat Basin is illustrated in Figure 2.2.

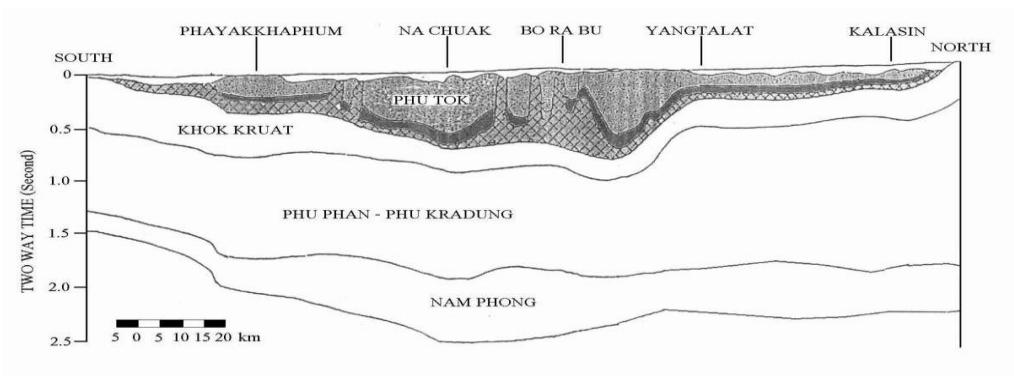


Figure 2.2 Cross-section showing rock salt in the Khorat Basin (Sattayarak, 1985).

2.3 Water Treatment Sludge from WMA

Adamant et al. (2006) determined the mechanical and durability of mortar to replace cement with dry sludge ash from Bang Khen water treatment plant. This research studied the chemical compositions and physical properties of the dry sludge ash, including the flow value and compressive strength. Durability against the sulfuric attack which is tested by using a sulfuric solution with pH of 1.0 and sodium sulfate (Na_2SO_4). Binder materials containing various proportions between the sludge ash and Portland cement, 0, 10, 20 and 30% by weight are prepared with the water to the binder material ratios of 0.50, 0.55 and 0.60. The results indicate that the dry sludge ash increased with decreasing flow value, compressive strength, and weight loss due to sulfuric acid attack.

Suriyachat et al. (2004) studied the basic properties of the water treatment sludge. The results indicate that the liquid limit is 77.96%, plastic limit is 50.76%, shrinkage limit is 11.15%, the plasticity index is 27.20% and the maximum density is

1.33 g/cm³. The correlation between permeability coefficient and the moisture content was found when the moisture content is low with high permeability coefficient. This is probably a result of a rearrangement of molecules at the particle surfaces by the action of adsorbing water leading to a formation of gain-soil bridges. The optimum moisture content of 29% is suitable for the minimum coefficient of permeability. The coefficient of permeability is similarly to the clay used in the ceramic industry.

The chemical compositions of the sludge and clay from the pottery in central and northern parts of Thailand suggest that the sludge properties are similar to the clay properties of these manufacturers. The analysis of chemical compositions showed that the amount of Fe₂O₃ was between 4 and 5%, including the optimal values of SiO₂ and Al₂O₃ as it is similar to red clay. This is an important raw material used in the ceramic industry.

Laboratory experiments in ceramic product made of the sludge are in the areas of pottery and jewelry. Those must be mixed with sand. To obtain a beautiful shape it must have the sand portion of 30%, but it takes several times for fermentation of the clay. The initially result showed that the water treatment sludge could be used as a raw material in the ceramic industry. Addition, it makes to achieve a renewable and reused in the manufacturing of integrated and sustainable natural materials.

Valls et al. (2004) has studied physical and mechanical properties of concrete mixed sludge. The sludge has used mixed component in construction materials an addition to plain concrete and studied four percentages of sludge mixed cement: concrete or 0% sludge; 2.5% sludge; 5% sludge; 10% sludge. The experiment indicated, the porosity tended to decrease, strength increased as the age of the

concrete increased from 7 to 90 days and elastic modulus decrease to the sludge content at 90 days.

2.4 Flow ability of grouting slurry

Rahmani (2004) explained that grouting had been used over the past two centuries to increase the strength, decrease the deformation and reduce the permeability of soils or fractured rocks. Due to its significance in engineering and science predicting grout effectiveness in fractured rocks was of interest. There were different approaches to estimate the effectiveness of grouting, one of which was numerical modeling. Numerical models could simulate a distribution of grout inside fractures by which the effectiveness of grout could be estimated. Few numerical studies had been carried out to model grout penetration in fractured rocks. Due to complexities of modeling grout and fracture most of these studies had either used simplifying assumptions or been bound to small sizes of fractures, both resulting in unrealistic simulations.

Then the current work is aimed to eliminate some of the simplifying assumptions and to develop a model that could improve the reliability of the results. In reality, grouts were believed to behave as a Bingham fluid, but many models did not consider a full Bingham fluid flow solution due to its complexity. Real fractures had rough surfaces with randomly varying apertures. However, some models considered fractures as planes with two parallel sides and a constant aperture. In this work the Bingham fluid flow equations were solved numerically over a stochastically varying aperture fracture. To simplify the equations and decrease the computational time the current model substituted two-dimensional elements by one-dimensional

pipes with equivalent properties. The model was capable of simulating the time penetration of grout in a mesh of fracture over a rather long period of time.

The results of the model could be used to predict the grout penetration for different conditions of fractures or grout (Rahmani, 2004).

2.5 Permeability of grout

The main factors controlling fluid flow through a single fracture are the surface roughness, apertures, orientation of fractures, normal and shear stresses, and unloading behavior. Out of these controlling factors, the aperture is the major parameter, which is a function of external stress, fluid pressure and geometrical properties of the fracture (Indraratna and Ranjith, 2001).

The conductivity of a single fracture is given by the ‘cubic law’: (Indraratna and Ranjith, 2001)

$$K_f = ge^3/12vb \quad (2.1)$$

where K_f = fracture conductivity (m/s), e = hydraulic aperture (m), g = acceleration due to gravity (m/s^2), ν = kinematic viscosity, which is 1.01×10^{-6} (m^2/s) for pure water at $20^\circ C$ and b is the spacing between fracture (m).

For a smooth, planar joint having an aperture of magnitude e , the fracture permeability (k) for laminar flow is given by (Barton et al., 1985)

$$k = e^2/12 \quad (2.2)$$

The joint aperture e is mainly dependent on the normal and shear stress acting on the joint. Assuming the rock matrix to be isotropic and linear elastic, obeying

Hooke's law, the following aperture-stress relationship can be formulated: (Indraratna and Ranjith, 2001)

$$e = e_0 \pm \delta e \quad (2.3)$$

where e_0 is the initial joint aperture and δe is the change of the joint aperture due to stresses (i.e., both normal and shear components) acting on the joint. In conventional rock mechanics, the normal deformation component is given by Jaeger and Cook (1979):

$$\delta e_n = (1/K_n)(\sigma_z \cos \beta + \sigma_h \sin \beta) \quad (2.4)$$

where K_n = normal stiffness of discontinuity, σ_z = vertical stress applied to the discontinuity, σ_h = horizontal stress applied to the discontinuity, and β = orientation of discontinuity.

Considering the water pressure to be acting perpendicular to the joint surface, the equation can be modified to obtain (Indraratna and Ranjith, 2001)

$$\delta e_n = (1/K_n)(\sigma_1 \cos \beta - \sigma_3 \sin \beta - p_w) \quad (2.5)$$

where p_w = water pressure within the discontinuity.

Combining the above equations for planar and smooth joints, the permeability of a single fracture is given by

$$k = (e_0 + \delta e_n)^2 / 12 \quad (2.6)$$

Based on the initial hydraulic aperture and the closure of joint, Detoumay (1980) suggested the following relationship to determine the fracture permeability:

$$k = e_0^2(1 - \nu/\nu_0)^2/12 \quad (2.7)$$

where e_0 = hydraulic aperture at zero stress, ν_0 = closure of the joint when the hydraulic aperture becomes zero and ν = normal deformation of the joint.

Snow (1968) observed an empirical model to describe the fracture fluid flow variation against the normal stress, as described by

$$k = k_0 + K_n(e^2/s)(\sigma - \sigma_0) \quad (2.8)$$

where k_0 = initial fracture permeability at initial normal stress (σ_0), K_n = normal stiffness, s = fracture spacing and e = hydraulic aperture.

Jones (1975) suggested the following empirical relation between the fracture permeability and the normal stress:

$$k = C_0[\log(\sigma_{ch}/\sigma_c)]^3 \quad (2.9)$$

where σ_{ch} = confining healing pressure in which the permeability is zero and σ_c = effective confining stress. The constant (C_0) depends on the fracture surface and the initial joint aperture.

Nelson (1975) suggested the following empirical relation between the fracture permeability and the normal stress:

$$k = A + B\sigma_c^{-m} \quad (2.10)$$

where A , B and m are constants which are determined by regression analysis. These constants may vary from one rock to another, and even for the same rock type, depending on the topography of the fracture surface.

Gangi (1978) reports a theoretical model for fracture permeability as a function of the confining pressure, as represented by

$$k = k_0[1 - (\sigma_c/P_I)^m]^3 \quad (2.11)$$

where P_I = effective modulus of the asperities and m = constant which describes the distribution function of the asperity length. This expression gives a better prediction if the effect of surface roughness on flow is negligible, which of course is not reasonable in practice.

2.6 Strength of cured grout

Owaidat et al. (1999) reported that the U.S. Army Corps of Engineers had recently implemented a levee-strengthening program along the banks of the American River in Sacramento, California. During the rainy season, the existing levee system protected major commercial and residential areas of this metropolitan area. One of the main components of this program was the construction of slurry walls through the existing levee to improve stability by preventing seepage through and beneath the levee. Since conventional soil-bentonite (SB) slurry walls had little shear strength, which would jeopardize the stability, of the existing levees and cement-bentonite (CB) slurry walls were significantly more expensive, soil-cement-bentonite (SCB) slurry walls were being utilized for this strengthening program. This research described a case study on the design, construction and performance of an underground SCB barrier wall, which was used to isolate river water seeping into the American River levee and its foundation soils. Challenges to barrier performance included

achieving a maximum allowable hydraulic conductivity of 5×10^{-7} cm/s while having a minimum unconfined compressive strength of 15 psi.

Kashir and Yanful (2000) reported that the use of slurry walls to contain oxidized tailings and provide cutoff below tailings dams were generally a cost-effective way of preventing environmental degradation due to seepage of acid water from tailing's areas. Long-term environmental protection dictated that the slurry wall materials been compatible with the acid water. Six percent bentonite by weight was added separately to two natural soils to represent slurry wall backfill materials, which were then permeated with several pore volumes of acid mine drainage (AMD) in the laboratory. Results using both flexible wall and fixed wall permeameters were similar. The carbonate-rich backfill gave an average hydraulic conductivity (K) of 1×10^{-9} cm/s, buffered the AMD at circumneutral pH, and kept effluent metal concentrations to very low values, for example, less than 0.05 mg/l zinc. The carbonate-free backfill also maintained low K (average 3×10^{-9} cm/s) during AMD permeation, it could not neutralize the AMD as effluent pH decreased to approximately 3.5 and metal concentrations reached those of the influent or permeant after about 17 pore volumes.

Rahmani (2004) explained that grouting had been used over the past two centuries to increase the strength, decrease the deformation and reduce the permeability of soils or fractured rocks. Due to its significance in engineering and science predicting grout effectiveness in fractured rocks was of interest. There were different approaches to estimate the effectiveness of grouting, one of which was numerical modeling. Numerical models could simulate a distribution of grout inside fractures by which the effectiveness of grout could be estimated. Few numerical

studies had been carried out to model grout penetration in fractured rocks. Due to complexities of modeling grout and fracture most of these studies had either used simplifying assumptions or been bound to small sizes of fractures, both resulting in unrealistic simulations.

Then the current work is aimed to eliminate some of the simplifying assumptions and to develop a model that could improve the reliability of the results. In reality, grouts were believed to behave as a Bingham fluid, but many models did not consider a full Bingham fluid flow solution due to its complexity. Real fractures had rough surfaces with randomly varying apertures. However, some models considered fractures as planes with two parallel sides and a constant aperture. In this work the Bingham fluid flow equations were solved numerically over a stochastically varying aperture fracture. To simplify the equations and decrease the computational time the current model substituted two-dimensional elements by one-dimensional pipes with equivalent properties. The model was capable of simulating the time penetration of grout in a mesh of fracture over a rather long period of time. The results of the model could be used to predict the grout penetration for different conditions of fractures or grout (Rahmani, 2004).

Butron et al. (2010) presented a new pre-excavation grouting concept to prevent dripping and reduced the inflow into a railway tunnel. For this purpose, the tunnel's roof was driped-sealed using colloidal silica and the walls and invert of the tunnel were grouted with cement. The grouting design process followed a structured approach with pre-investigations of core-drilled boreholes providing parameters for the layout. Water pressure tests and pressure volume time recordings were used for the evaluation. Results showed that the design was successful: the total transmissivity

was reduced from $4.9 \times 10^{-8} \text{ m}^2/\text{s}$ to the measurement limit ($1.6 \times 10^{-8} \text{ m}^2/\text{s}$), and the dripping was reduced to eight spots from the roof. Improved rock characterization showed that the grout hole separation was within the transmissivity correlation length and that grouting efficiency depends to a large extent on the dimensionality of the flow system of the rock mass.



CHAPTER III

CEMENT GROUT AND ROCK SALT SPECIMEN PREPARATION

3.1 Cement Grout Preparation

The sludge-mixed cement mixing is performed according to API NO.10 (American Petroleum Institute, 1986; Akgun and Daemen, 1997) by mixing cement with sludge (particle size less than 0.0075 mm) and salt (NaCl) saturated brine. The components of sludge-mixed cement slurry are commercial grade Portland cement mixed with chloride resistant agent (Portland-pozzolan cement, type IP), sludge, NaCl saturated brine and anti-form agent. The brine is prepared either by dissolving clean rock salt in distilled water. Anti-form agent is used to decrease the air content of the cement of the cement sludge and ease to control of the cement slurry weight and volume. Table 1 gives the weight composition of mixture. Sludge is tested for the Atterberg's limits, specific gravity, and particle size distribution. The equipment and test procedure follow the ASTM standards (D422, D854). The average liquid limit, plastic limit and plasticity index are 55%, 22% and 23%, respectively. The average specific gravity is 2.56. Figure 3.1 shows the particle size distributions of the sludge used here (Wetchasat and Fuenkajorn, 2012). All grouts are prepared by mixing at the brine-to-sludge -mixed cement ratio of 1:1. The saturated brine is poured into the mixing container at a low mixture speed, and all components are added to the brine within 15 seconds. After all the cement is added, the slurry is mixed at high speed for additional 35 seconds. The cement

slurry mixtures are poured and cured in 54 mm diameter PVC mold for the mechanical characterization test. Molds are cured under atmospheric pressure at room temperature (28 to 30°C). Figure 3.2 and 3.3 show some of specimen prepared for uniaxial compressive strength test and Brazilian tensile strength test, respectively. Over 240 specimens are prepared for testing.

3.2 Rock salt specimen

Core 54 mm diameter samples of salt are donated by Pimai Salt Company Limited, Nakhon Ratchasima province. They are collected from borehole located Pimai district. All samples are obtained from the Middle Salt members at depths between 30 m and 70 m in Khorat basin. Sample preparation are followed the ASTM D4543 standard practice, as much as practical. Six specimens are prepared for push-out tests with length about 100 mm. After preparation, the specimens are labeled and wrapped with plastic film. The specimen designation is identified. The petrographic properties of the tested cores are as follows. The salt crystals are tightly interlocked. The diameters of milky white halite range from 0.1 to 0.2 cm. Smoky dark halite is associated with anhydrite and clay inclusions. The associated minerals include local occurrence of carnallite. Some large crystals ranging from 2.0 to 3.0 cm are locally occurred. Figure 3.4 shows plug with 54 mm diameter of rock salt specimen prepared within the PVC mold for push-out tests.

Table 3.1 Weight composition of sludge-mixed cement slurry.

Specimen Type	Mix ratio	Density (g/cc)	color	Composition of slurry (g)		
				Cement (g)	Brine (g)	Sludge (g)
Cement	0:10	1.56	gray	68.77	68.77	0
SC 0.1	1:10	1.65	brownish	63.94	63.94	6.39
SC 0.2	2:10	1.71	brownish	59.74	59.74	11.95
SC 0.3	3:10	1.72	brownish	56.06	56.60	16.82
SC 0.4	4:10	1.73	sable	52.81	52.81	21.12
SC 0.5	5:10	1.75	sable	49.91	49.91	24.96

(Density of cement is 1.56 g/cc, brine is 1.23 g/cc and sludge is 0.91 g/cc)

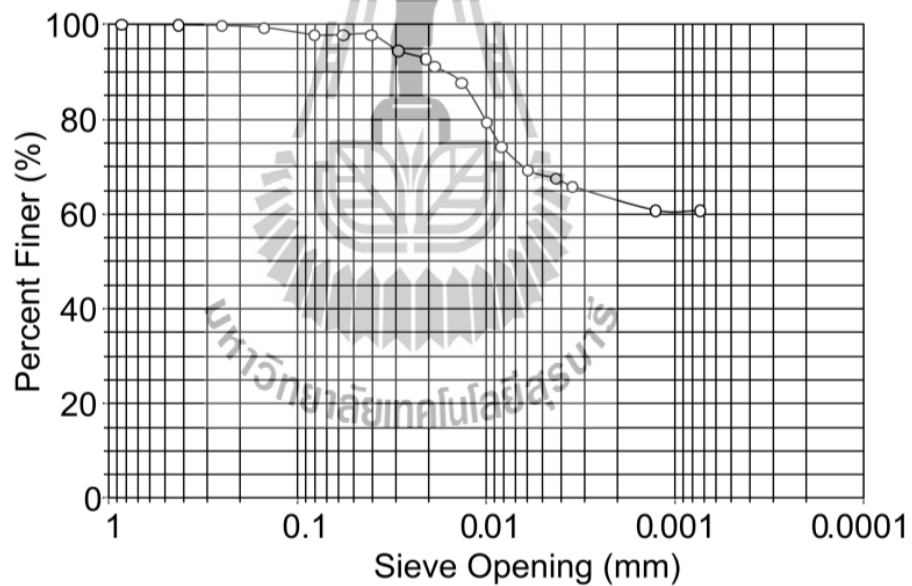


Figure 3.1 Grain size distribution of water treatment sludge. (Wetchasat and Fuenkajorn, 2013)



Figure 3.2 Sludge-mixed concrete specimens prepared for uniaxial compressive strength test having 54 mm in diameter with L/D ratio of 2.5.

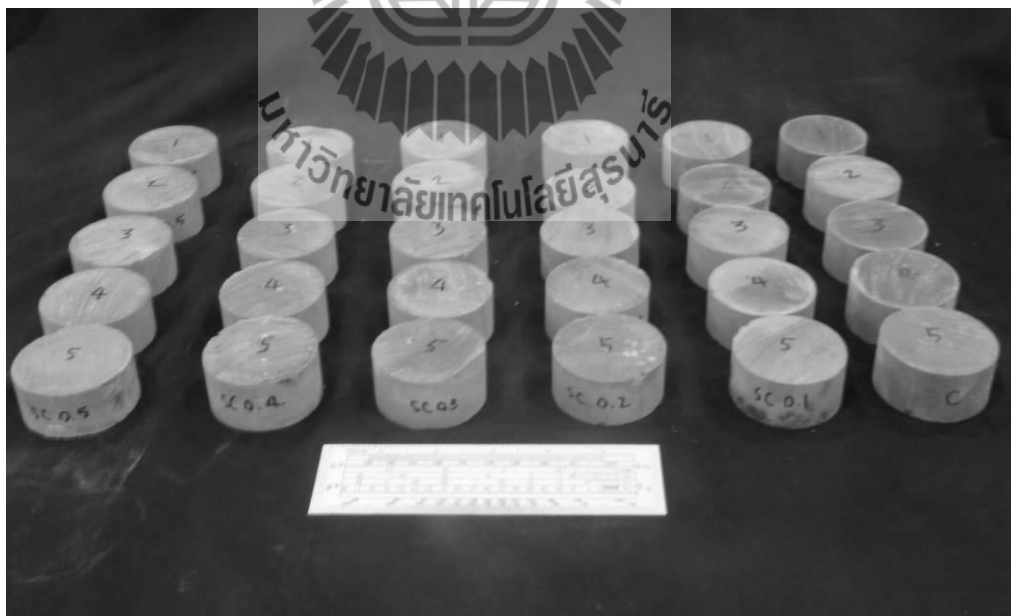


Figure 3.3 Sludge-mixed concrete specimens prepared for Brazilian tensile strength test having 54 mm in diameter with L/D ratio of 0.5.

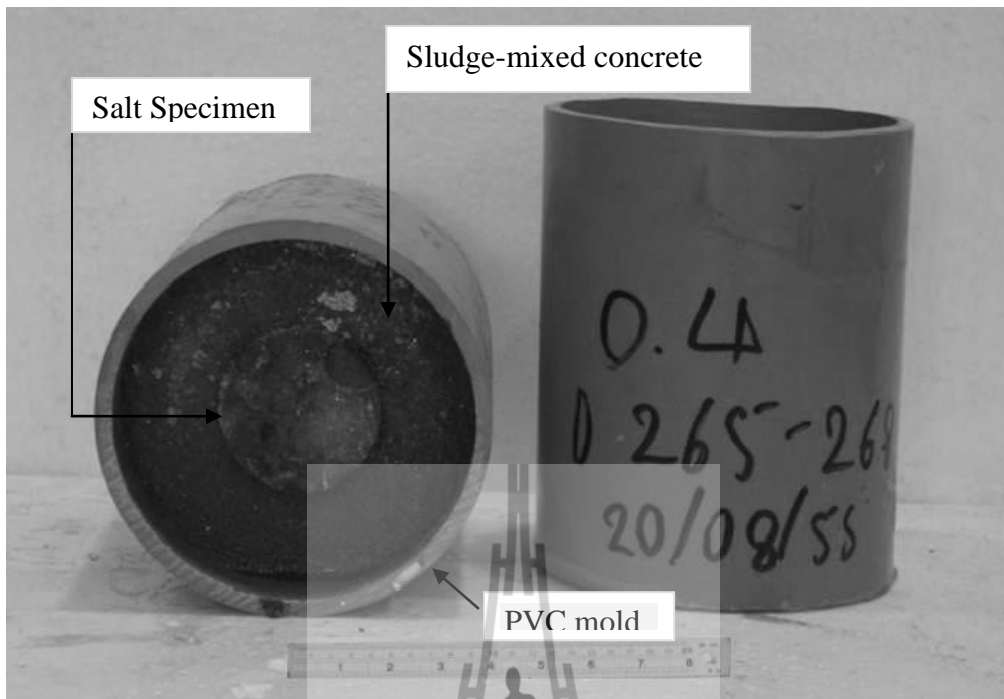


Figure 3.4 Salt specimens are placed into the inner borehole of sludge-mixed cement cylinder within the PVC mold for push-out tests.



CHAPTER IV

LABORATORY TESTING

4.1 Introduction

The objective of the laboratory testing is to study the mechanical and hydraulic performance assessment of sludge-mixed cement grout in salt fractures under brine and balance of concrete mixed brine ratios. This chapter describes the method and results of the laboratory testing. The tests are divided into three groups including 1) basic mechanical characterization tests of grouting material, 2) push-out resistance tests and 3) permeability tests of grouting materials.

4.2 Basic Mechanical Characterization of Grouting Materials

The basic mechanical properties of the mixtures are determined to select the appropriate proportions of sludge-to-cement ratios. The sludge-mixed cement ratios (S:C) 0:10, 1:10, 2:10, 3:10, 4:10 and 5:10 by weight are prepared with brine-sludge-mixed cement ratio of 1:1. Characterization testing provides the viscosity and slurry density of cement grout, the uniaxial compressive strength (σ_c), Young's modulus (E) and Brazilian tensile strength (σ_B),

4.2.1 Viscosity and Density of Cement Slurry

The flow ability is an important parameter related to the grout mixture proportions. The flow of sludge-mixed cement grout is measured by determine its viscosity and density. The viscosity test follows, as much as practical, ASTM D2196. The density test follows the ASTM D854 standard practical. The grout preparation follows the ASTM C938 standard practice. The viscosity is measured with Brookfield ® viscometer (model RV) using a Hobart type laboratory mixture (Figure 4.1). The measurement is followed;

- 1) The grout slurry mixtures are poured in 500 ml-beaker.
- 2) Weighing of grout slurry mixtures and record.
- 3) Calculate the density of grout slurry.
- 4) Install the beaker of grout slurry mixture in viscometer.
- 5) Measure the viscosity.

Testing is performed at room temperature and atmospheric pressure following standard ASTM D2196 and ASTM D854.

Table 4.2 shows results of six viscosity and density measurements with sludge-mixed cement ratios (S:C) 0:10, 1:10, 2:10, 3:10, 4:10 and 5:10, respectively. The dynamics viscosity of cement slurries tends to increase as the sludge-mixed cement ratio increase. The highest viscosity and density are occurred in mixed ratio of S:C = 5:10. This ratio of grout mixture proportion is selected to study the push-out resistance with rock salt specimens.

Table 4.1. Viscosity and slurry density of cement slurry.

Type	Mix ratio	Temperature (°C)		Cement Slurry Density (g/cc)	Dynamic Viscosity ($\times 10^3$ mPa·s)
		Room	Slurry		
C	0:10	30.1	27.4	1.56	1.27
S:C	1:10	31.0	28.0	1.65	1.07
S:C	2:10	30.2	28.0	1.71	1.33
S:C	3:10	30.4	28.5	1.72	1.53
S:C	4:10	29.5	27.5	1.73	1.59
S:C	5:10	30.2	27.8	1.75	2.28

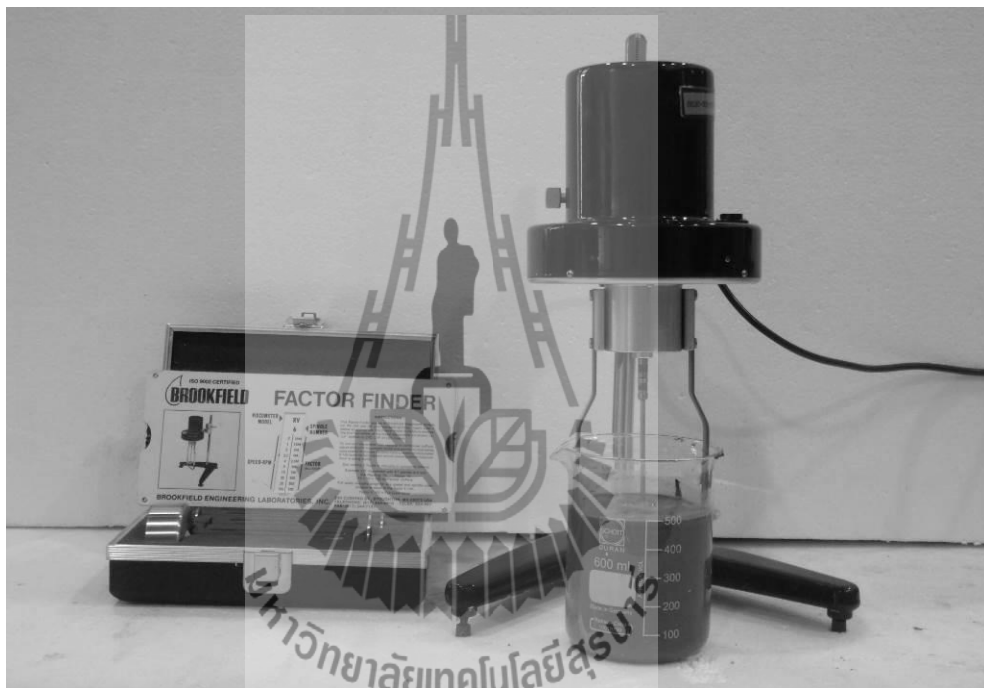


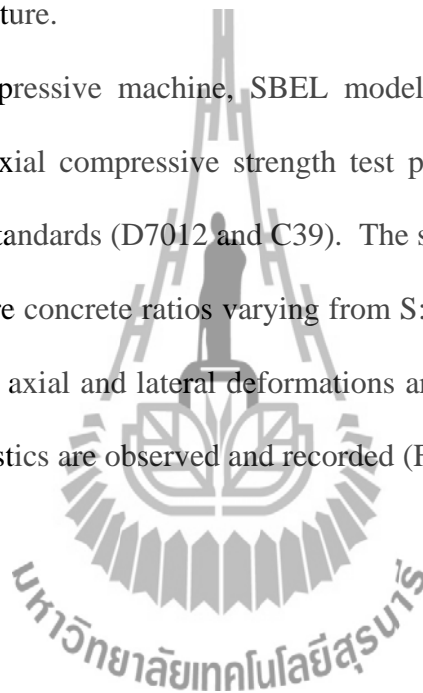
Figure 4.1 Measurement of the viscosity of sludge-mixed cement slurry with Brookfield ® viscometer model RV (ASTM D2196).

4.2.2 Uniaxial Compressive Strength Testing

The objective of the uniaxial compressive strength tests is to determine the ultimate strength and ability of the concrete specimens under uniaxial compression at various ratios admixture of cements. The test procedures follow the American Society for Testing and Materials (ASTM C938, D4832 and C39). One

hundred and eight of 54 mm diameter cylindrical sludge-mixed cement specimens with length to diameter (L/D) ratios between 2.0 and 3.0 are prepared by curing cement pastes in PVC molds for 7, 14, 21, and 28 days, respectively. Each mold is puddled with the puddling rod to eliminate cement segregation. The remaining portion of the molds is filled with brine. All cement cylinders are taken out of their molds after each curing period. The ends of specimen are cut and paralleled. They are cured at room temperature.

A compressive machine, SBEL model PLT-75 is used to load the specimens. The uniaxial compressive strength test procedure follows, as much as practical, the ASTM standards (D7012 and C39). The specimens are loaded axially to failure under admixture concrete ratios varying from S:C = 1:10, 2:10, 3:10, 4:10 and 5:10. During test, the axial and lateral deformations are monitored (Figure 4.2). The post-failure characteristics are observed and recorded (Figure 4.3).



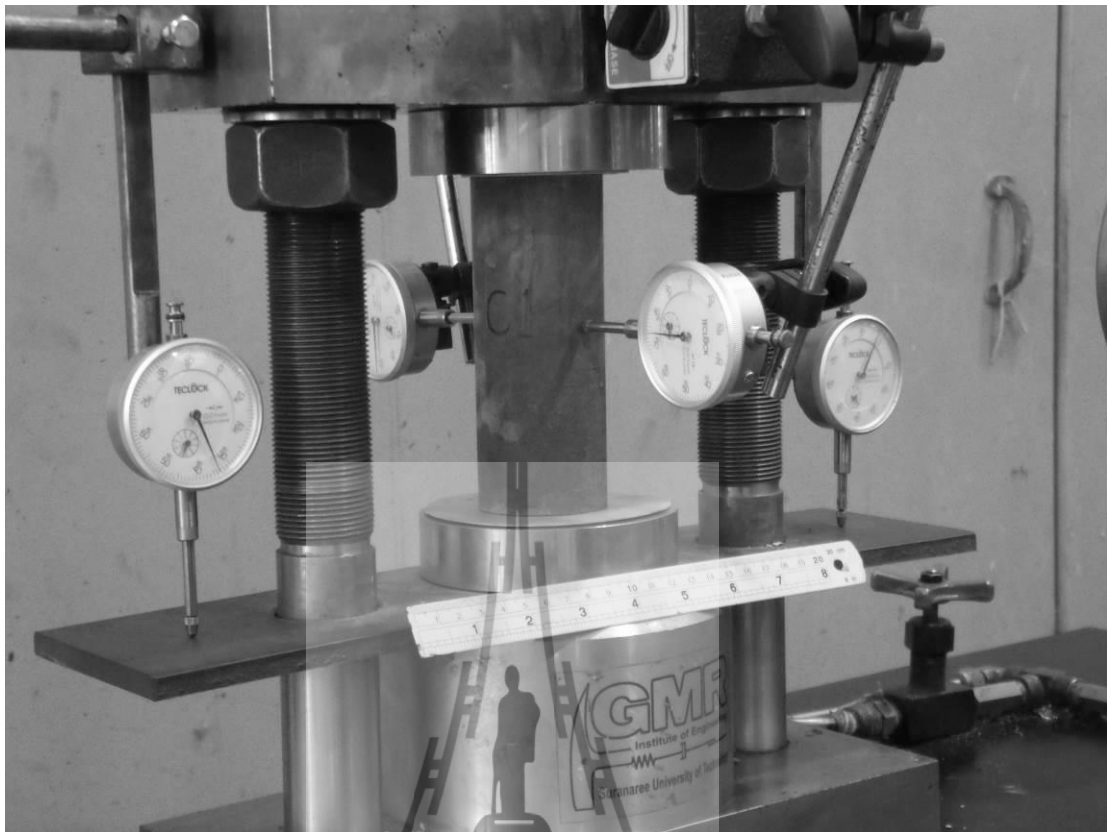


Figure 4.2 Uniaxial compressive strength test on 54 mm diameter specimen of sludge-mixed cement with L/D ratio 2.5

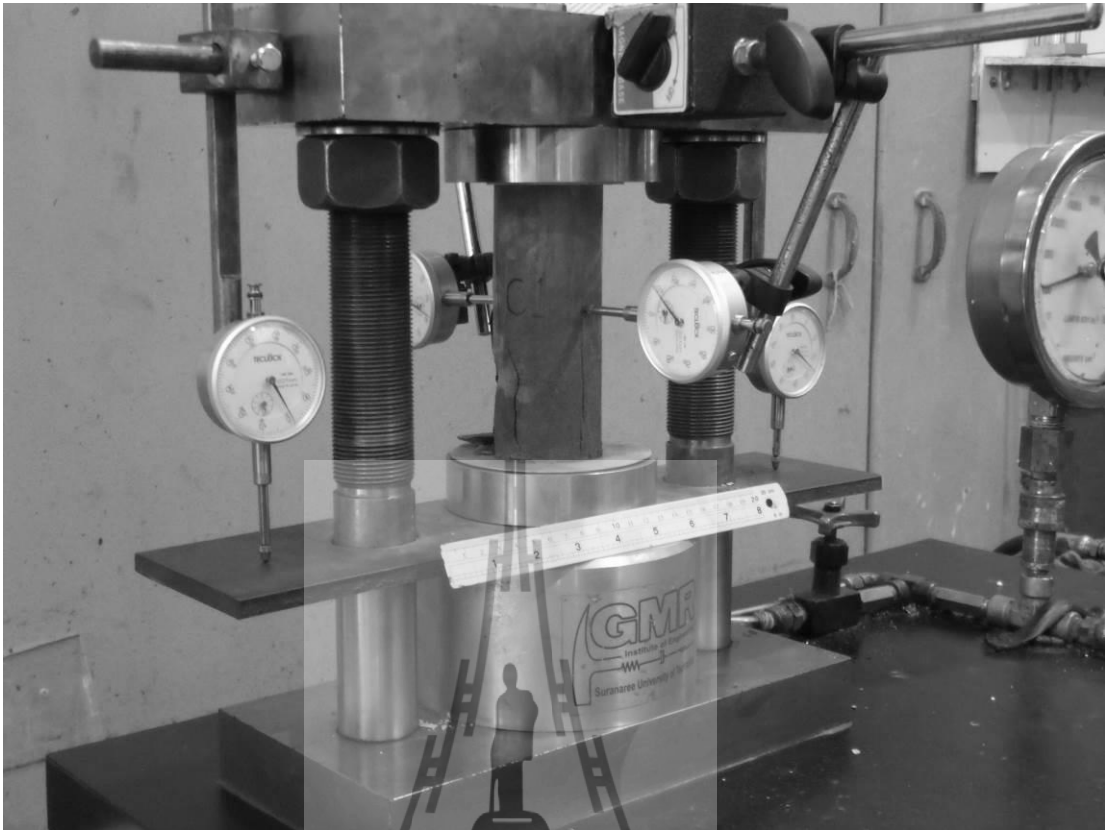


Figure 4.3 Specimen failed by uniaxial compressive strength test.

The results of uniaxial compressive strength are shown in Table 4.2 through Table 4.7. Figure 4.4 plots the uniaxial compressive strength as a function of curing time obtained from the uniaxial compressive strength under various admixture of sludge-mixed cement. Despite the intrinsic change among the specimens the curves tend to show loading dependent behavior of the admixture of concretes. The tangent elastic moduli at failure stress have been calculated from the measured stress-strain curves obtained from all uniaxial specimens (Figure 4.5). They tend to be increases with specimen case. Post-test observations indicate that under varies admixture of sludge-mixed cement, all of the specimens experienced splitting failure.

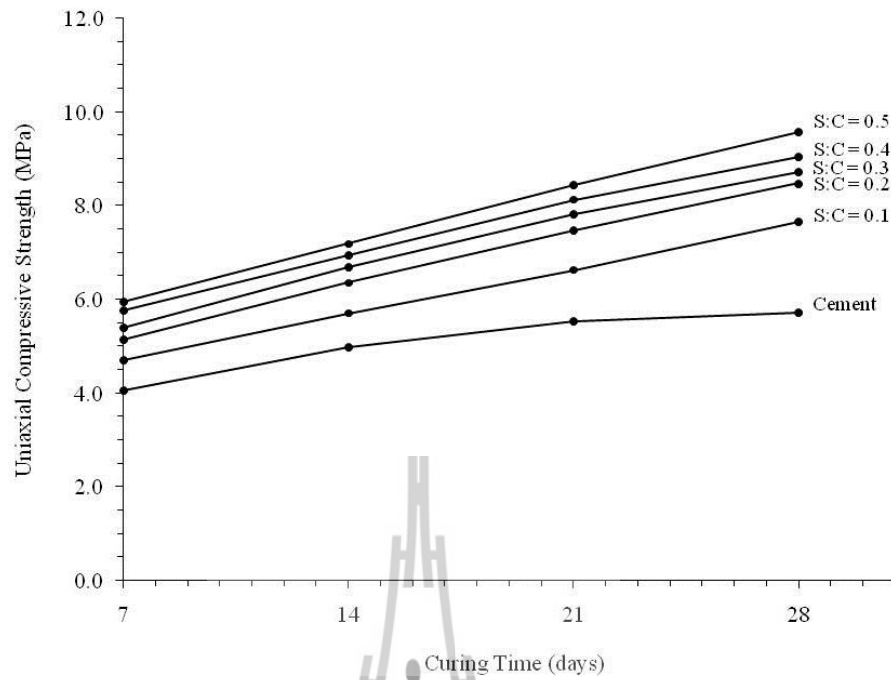


Figure 4.4 Uniaxial compressive strength of sludge-mixed cement as a function of curing time.

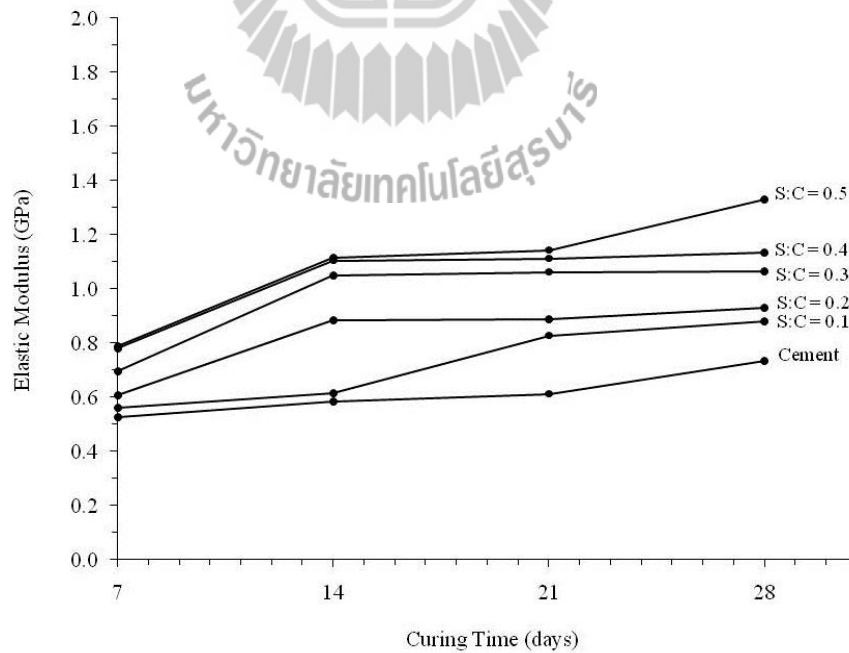


Figure 4.5 Elastic modulus of sludge-mixed cement as a function of curing time.

Table 4.2 Uniaxial compressive strength and elastic modulus of grouting material (S:C = 0:10).

Admixture	Curing time (day)	Demeter (mm)	Length (mm)	L/D	Density (g/cc)	Average (g/cc)	UCS (MPa)	Average (g/cc)	Elastic Modulus (GPa)	Average (g/cc)
C-07-UCS-01	7	54.00	126.00	2.33	1.07	1.07	4.70	4.05	0.44	0.52
C-07-UCS-02		54.00	134.00	2.48	1.06		3.90		0.59	
C-07-UCS-03		54.52	138.24	2.54	1.07		3.00		0.58	
C-07-UCS-04		54.32	135.10	2.49	1.07		4.60		0.49	
C-14-UCS-01	14	54.00	135.00	2.50	1.08	1.08	4.40	4.98	0.51	0.58
C-14-UCS-02		54.00	135.00	2.50	1.07		4.89		0.56	
C-14-UCS-03		54.00	135.00	2.50	1.10		4.40		0.58	
C-14-UCS-04		54.00	135.00	2.50	1.08		5.40		0.63	
C-14-UCS-05		54.00	135.00	2.50	1.08		5.80		0.64	
C-21-UCS-01	21	54.72	135.70	2.48	1.17	1.10	5.20	5.54	0.62	0.61
C-21-UCS-02		54.26	137.96	2.54	1.07		6.10		0.64	
C-21-UCS-03		54.68	137.96	2.52	1.07		4.30		0.51	
C-21-UCS-04		55.00	136.82	2.49	1.07		5.20		0.64	
C-21-UCS-05		54.35	137.00	2.52	1.13		6.90		0.66	
C-28-UCS-01	28	54.00	136.00	2.52	1.10	1.10	5.20	5.73	0.71	0.74
C-28-UCS-02		54.00	135.90	2.52	1.07		6.50		0.74	
C-28-UCS-03		53.45	136.68	2.56	1.08		4.90		0.75	
C-28-UCS-04		53.40	137.20	2.57	1.16		6.30		0.74	

Table 4.3 Uniaxial compressive strength and elastic modulus of grouting materials (S:C = 1:10).

Admixture	Curing time (day)	Demeter (mm)	Length (mm)	L/D	Density (g/cc)	Average (g/cc)	UCS (MPa)	Average (g/cc)	Elastic Modulus (GPa)	Average (g/cc)
SC0.1-07-UCS-01	7	107.46	206.38	1.92	1.11	1.11	4.50	4.70	0.42	0.56
SC0.1-07-UCS-02		107.26	206.98	1.93	1.13		4.50		0.63	
SC0.1-07-UCS-03		106.08	203.96	1.92	1.10		5.10		0.63	
SC0.1-14-UCS-01	14	54.00	139.00	2.57	1.10	1.11	5.70	5.71	0.59	0.61
SC0.1-14-UCS-02		54.22	135.30	2.50	1.11		5.60		0.62	
SC0.1-14-UCS-03		54.46	135.60	2.49	1.11		6.01		0.71	
SC0.1-14-UCS-04		54.30	137.24	2.53	1.12		5.20		0.52	
SC0.1-14-UCS-05		54.40	138.14	2.54	1.11		6.02		0.63	
SC0.1-21-UCS-01	21	53.92	116.83	2.17	1.12	1.12	5.69	6.63	0.55	0.83
SC0.1-21-UCS-02		54.71	126.28	2.31	1.12		7.66		0.94	
SC0.1-21-UCS-03		55.00	138.74	2.52	1.13		4.21		0.56	
SC0.1-21-UCS-04		54.12	136.52	2.52	1.12		8.69		1.01	
SC0.1-21-UCS-05		54.32	135.90	2.50	1.11		6.90		1.09	
SC0.1-28-UCS-01	28	53.80	134.91	2.51	1.12	1.12	7.04	7.67	0.88	0.99
SC0.1-28-UCS-02		53.30	130.50	2.45	1.12		8.10		0.84	
SC0.1-28-UCS-03		54.00	134.50	2.49	1.13		7.40		1.10	
SC0.1-28-UCS-04		54.15	133.20	2.46	1.13		9.10		1.00	
SC0.1-28-UCS-05		53.40	135.00	2.53	1.12		6.70		1.12	

Table 4.4 Uniaxial compressive strength and elastic modulus of grouting materials (S:C = 2:10).

Admixture	Curing time (day)	Demeter (mm)	Length (mm)	L/D	Density (g/cc)	Average (g/cc)	UCS (MPa)	Average (g/cc)	Elastic Modulus (GPa)	Average (g/cc)
SC0.2-07-UCS-01	7	106.60	207.66	1.95	1.14	1.14	4.50	5.13	0.82	0.61
SC0.2-07-UCS-02		107.20	206.90	1.93	1.13		5.50		0.57	
SC0.2-07-UCS-03		108.22	203.96	1.88	1.15		5.40		0.42	
SC0.2-14-UCS-01	14	54.00	127.00	2.35	1.14	1.14	6.48	6.36	0.92	0.88
SC0.2-14-UCS-02		54.00	135.00	2.50	1.13		6.10		0.91	
SC0.2-14-UCS-03		54.00	127.00	2.35	1.14		5.70		0.72	
SC0.2-14-UCS-04		54.00	127.00	2.35	1.15		7.00		0.91	
SC0.2-14-UCS-05		54.30	138.50	2.55	1.15		6.50		0.96	
SC0.2-21-UCS-01	21	53.91	116.78	2.17	1.16	1.17	7.90	7.48	1.13	0.89
SC0.2-21-UCS-02		53.71	136.21	2.54	1.16		7.10		1.02	
SC0.2-21-UCS-03		53.71	136.38	2.54	1.16		7.50		0.42	
SC0.2-21-UCS-04		53.84	136.68	2.54	1.19		6.98		1.02	
SC0.2-21-UCS-05		54.00	136.18	2.52	1.16		7.90		0.85	
SC0.2-28-UCS-01	28	53.98	135.30	2.51	1.19	1.18	5.68	8.48	0.75	1.00
SC0.2-28-UCS-02		54.10	135.32	2.50	1.19		10.01		0.99	
SC0.2-28-UCS-03		54.00	135.80	2.51	1.19		7.42		0.96	
SC0.2-28-UCS-04		54.00	134.00	2.48	1.16		7.86		0.99	
SC0.2-28-UCS-05		53.80	136.38	2.53	1.17		11.44		1.30	

Table 4.5 Uniaxial compressive strength and elastic modulus of grouting materials (S:C = 3:10).

Admixture	Curing time (day)	Demeter (mm)	Length (mm)	L/D	Density (g/cc)	Average (g/cc)	UCS (MPa)	Average (g/cc)	Elastic Modulus (GPa)	Average (g/cc)
SC0.3-07-UCS-01	7	107.26	204.00	1.90	1.13	1.15	6.10	5.40	0.92	0.70
SC0.3-07-UCS-02		107.00	206.68	1.93	1.16		5.60		0.41	
SC0.3-07-UCS-03		106.60	202.56	1.90	1.17		4.50		0.76	
SC0.3-14-UCS-01	14	54.40	136.28	2.51	1.17	1.17	7.31	6.69	1.23	1.05
SC0.3-14-UCS-02		54.00	134.00	2.48	1.16		7.42		1.09	
SC0.3-14-UCS-03		54.10	135.50	2.50	1.17		6.50		1.06	
SC0.3-14-UCS-04		54.20	137.00	2.53	1.17		5.60		0.91	
SC0.3-14-UCS-05		53.80	135.00	2.51	1.16		6.60		0.96	
SC0.3-21-UCS-01	21	54.00	127.00	2.35	1.16	1.18	8.73	7.81	1.05	1.06
SC0.3-21-UCS-02		54.00	136.00	2.52	1.18		7.42		0.91	
SC0.3-21-UCS-03		54.00	135.52	2.51	1.18		7.90		1.08	
SC0.3-21-UCS-04		54.46	135.60	2.49	1.19		7.30		1.29	
SC0.3-21-UCS-05		54.46	126.88	2.33	1.17		7.70		0.98	
SC0.3-28-UCS-01	28	54.00	135.00	2.50	1.19	1.18	8.70	8.72	1.35	1.07
SC0.3-28-UCS-02		54.00	135.00	2.50	1.18		7.86		0.85	
SC0.3-28-UCS-03		54.00	135.00	2.50	1.19		9.56		1.22	
SC0.3-28-UCS-04		54.00	135.00	2.50	1.19		8.73		0.91	
SC0.3-28-UCS-05		54.00	135.00	2.50	1.18		8.73		1.00	

Table 4.6 Uniaxial compressive strength and elastic modulus of grouting materials (S:C = 4:10).

Admixture	Curing time (day)	Demeter (mm)	Length (mm)	L/D	Density (g/cc)	Average (g/cc)	UCS (MPa)	Average (g/cc)	Elastic Modulus (GPa)	Average (g/cc)
SC0.4-07-UCS-01	7	106.98	205.40	1.92	1.15	1.15	5.56	5.75	0.80	0.78
SC0.4-07-UCS-02		106.60	201.48	1.89	1.15		5.60		0.79	
SC0.4-07-UCS-03		107.86	205.72	1.91	1.16		6.10		0.76	
SC0.4-14-UCS-01	14	53.80	134.70	2.50	1.17	1.17	7.92	6.94	1.04	1.11
SC0.4-14-UCS-02		54.10	135.80	2.51	1.17		7.40		1.10	
SC0.4-14-UCS-03		54.40	135.30	2.49	1.17		7.31		1.12	
SC0.4-14-UCS-04		54.52	136.88	2.51	1.18		6.85		1.01	
SC0.4-14-UCS-05		54.00	135.90	2.52	1.17		5.24		1.26	
SC0.4-21-UCS-01	21	54.00	135.00	2.50	1.19	1.19	11.35	8.13	1.29	1.11
SC0.4-21-UCS-02		54.00	135.00	2.50	1.19		7.42		1.04	
SC0.4-21-UCS-03		54.00	135.00	2.50	1.18		7.90		0.97	
SC0.4-21-UCS-04		54.00	135.00	2.50	1.19		6.11		1.28	
SC0.4-21-UCS-05		54.00	135.00	2.50	1.18		7.86		1.00	
SC0.4-28-UCS-01	28	54.00	137.00	2.54	1.20	1.19	8.73	9.05	1.03	1.13
SC0.4-28-UCS-02		54.00	137.00	2.54	1.19		6.11		0.98	
SC0.4-28-UCS-03		54.00	136.00	2.52	1.18		8.30		1.11	
SC0.4-28-UCS-04		53.86	137.44	2.55	1.19		11.85		1.36	
SC0.4-28-UCS-05		54.56	138.28	2.53	1.19		10.27		1.18	

Table 4.7 Uniaxial compressive strength and elastic modulus of grouting materials. (S:C = 5:10).

Admixture	Curing time (day)	Demeter (mm)	Length (mm)	L/D	Density (g/cc)	Average (g/cc)	UCS (MPa)	Average (g/cc)	Elastic Modulus (GPa)	Average (g/cc)
SC0.5-07-UCS-01	7	107.46	208.44	1.94	1.16	1.16	5.50	5.95	0.80	0.79
SC0.5-07-UCS-02		107.00	205.90	1.92	1.15		6.25		0.78	
SC0.5-07-UCS-03		107.00	204.42	1.91	1.16		6.10		0.78	
SC0.5-14-UCS-01	14	54.40	136.60	2.51	1.16	1.18	6.94	7.19	1.12	1.12
SC0.5-14-UCS-02		54.48	135.70	2.49	1.17		6.86		1.09	
SC0.5-14-UCS-03		53.95	136.38	2.53	1.18		7.40		1.18	
SC0.5-14-UCS-04		54.42	135.50	2.49	1.18		7.74		1.12	
SC0.5-14-UCS-05		54.00	135.50	2.51	1.18		7.00		1.07	
SC0.5-21-UCS-01	21	54.50	135.00	2.48	1.18	1.19	8.12	8.45	1.08	1.14
SC0.5-21-UCS-02		54.00	134.00	2.48	1.20		8.65		1.19	
SC0.5-21-UCS-03		54.00	137.00	2.54	1.19		8.30		1.25	
SC0.5-21-UCS-04		54.00	137.00	2.54	1.19		7.93		1.16	
SC0.5-21-UCS-05		53.92	138.36	2.57	1.20		9.24		1.04	
SC0.5-28-UCS-01	28	54.00	137.00	2.54	1.20	1.20	9.10	9.58	1.32	1.33
SC0.5-28-UCS-02		54.00	137.00	2.54	1.20		9.52		1.43	
SC0.5-28-UCS-03		54.00	136.00	2.52	1.20		10.45		1.38	
SC0.5-28-UCS-04		53.86	137.44	2.55	1.20		9.25		1.26	
SC0.5-28-UCS-05		54.56	138.28	2.53	1.19		9.57		1.27	

4.2.3 Brazilian Testing

The objective of the Brazilian tensile strength test is to determine the indirect tensile strength of the sludge-mixed cement ratio S:C = 1:10, 2:10, 3:10, 4:10 and 5:10. The sample preparation and test procedure follow the applicable ASTM standard practice (ASTM D3967) and ISRM suggested method (Brown, 1981), as much as practical. One hundred and twenty samples with a diameter of 54 mm are tested with L/D 0.5. The test is performed by increasing the axial loaded at the constant rate of 0.1-0.5 MPa/second to sludge-mixed cement specimen until failure (Figure 4.6).



Figure 4.6 Brazilian test on 54 mm diameter specimen of sludge-mixed cement. The specimen is loaded along the diameter in SBEL PLT-75 loading machine.

(a) Pre-test specimen.



Figure 4.7 Post-tested specimen of Brazilian test.

The results of the Brazilian tensile strength tests are shown in Table 4.8 through 4.13. The tensile strength is calculated using the equation (Jaeger and Cook, 1979);

$$\sigma_B = \frac{2p_f}{\pi Dt} \quad (4.1)$$

where σ_B is the Brazilian test tensile strength, p_f is the failure load, D is the disk diameter, and t is the disk thickness. All specimens failed along the loading diameter (Figure 4.7). Figure 4.8 shows the average Brazilian strengths as function of curing time.

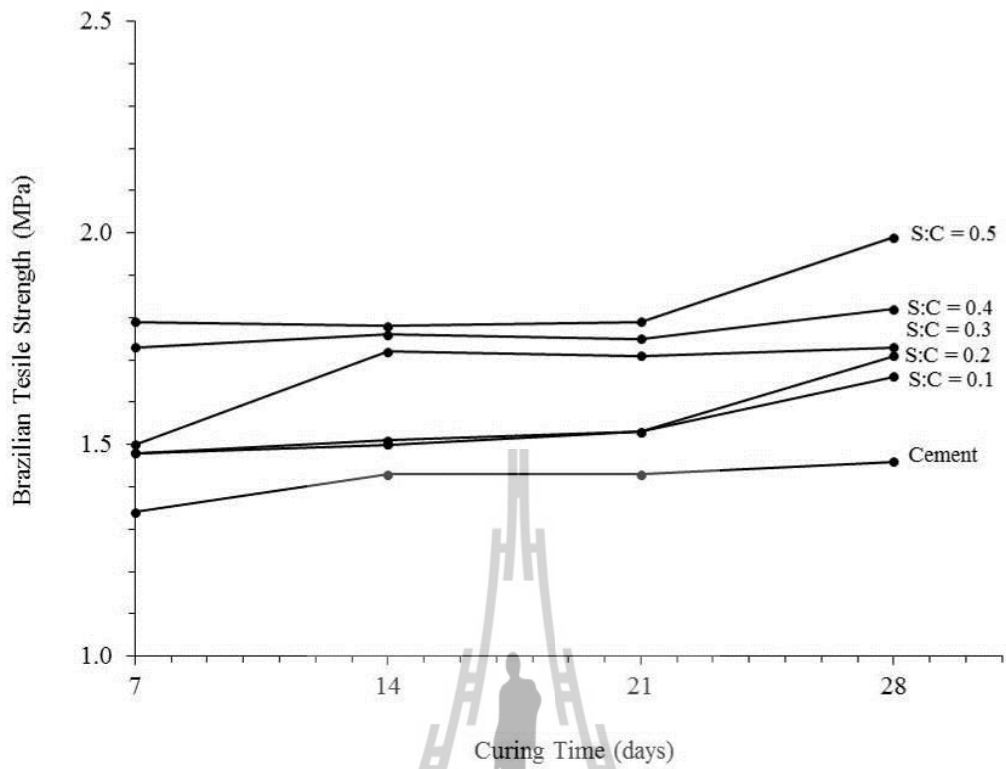


Figure 4.8 Brazilian tensile strength of sludge-mixed cement as a function of curing time.

มหาวิทยาลัยเทคโนโลยีสุรนารี

Table 4.8 Results of the Brazilian tensile strength testing with Specimen of S:C = 0:10.

Admixture	Curing time	Diameter (mm)	Thick (mm)	L/D	Density (g/cc)	Normal load (KN)	Tensile strength (MPa)
C-07-BZ-01	7	54.00	28.0	0.52	1.07	3.20	1.35
C-07-BZ-02	7	54.00	27.8	0.51	1.05	3.15	1.34
C-07-BZ-03	7	54.00	28.0	0.52	1.05	3.30	1.39
C-07-BZ-04	7	54.00	28.0	0.52	1.03	3.20	1.35
C-07-BZ-05	7	54.00	28.0	0.52	1.06	3.00	1.26
				Average	1.05	Average	1.34
C-14-BZ-01	14	54.00	27.5	0.51	1.07	3.40	1.46
C-14-BZ-02	14	54.00	27.8	0.51	1.06	3.30	1.40
C-14-BZ-03	14	54.00	28.0	0.52	1.06	3.50	1.47
C-14-BZ-04	14	54.00	28.0	0.52	1.05	3.40	1.43
C-14-BZ-05	14	54.00	28.0	0.52	1.06	3.30	1.39
				Average	1.06	Average	1.43
C-21-BZ-01	21	54.00	28.0	0.52	1.11	3.40	1.43
C-21-BZ-02	21	54.00	27.8	0.51	1.08	3.30	1.40
C-21-BZ-03	21	54.00	28.0	0.52	1.06	3.50	1.47
C-21-BZ-04	21	54.00	27.5	0.51	1.10	3.40	1.46
C-21-BZ-05	21	54.00	28.0	0.52	1.08	3.30	1.39
				Average	1.09	Average	1.43
C-28-BZ-01	28	54.00	27.5	0.51	1.07	3.50	1.50
C-28-BZ-02	28	54.00	27.8	0.51	1.11	3.10	1.32
C-28-BZ-03	28	54.00	26.4	0.49	1.08	3.60	1.61
C-28-BZ-04	28	54.00	27.7	0.51	1.11	3.35	1.43
C-28-BZ-05	28	54.00	28.8	0.53	1.06	3.50	1.43
				Average	1.09	Average	1.46

Table 4.9 Results of the Brazilian tensile strength testing with Specimen of S:C = 1:10.

Admixture	Curing time	Diameter (mm)	Thick (mm)	L/D	Density (g/cc)	Normal load (KN)	Tensile strength (MPa)
SC0.1-07-BZ-01	7	54.00	27.5	0.51	1.11	3.30	1.42
SC0.1-07-BZ-02	7	54.00	28.0	0.52	1.07	3.40	1.43
SC0.1-07-BZ-03	7	54.00	27.5	0.51	1.05	3.50	1.50
SC0.1-07-BZ-04	7	54.00	27.5	0.51	1.05	3.60	1.54
SC0.1-07-BZ-05	7	54.00	27.8	0.51	1.05	3.60	1.53
				Average	1.07	Average	1.48
SC0.1-14-BZ-01	14	54.00	27.0	0.50	1.10	3.30	1.44
SC0.1-14-BZ-02	14	54.00	28.0	0.52	1.09	3.60	1.52
SC0.1-14-BZ-03	14	54.00	27.5	0.51	1.07	3.50	1.50
SC0.1-14-BZ-04	14	54.00	27.5	0.51	1.06	3.50	1.50
SC0.1-14-BZ-05	14	54.00	27.7	0.51	1.09	3.60	1.53
				Average	1.08	Average	1.50
SC0.1-21-BZ-01	21	54.00	27.5	0.51	1.11	3.40	1.46
SC0.1-21-BZ-02	21	54.00	28.0	0.52	1.11	3.60	1.52
SC0.1-21-BZ-03	21	54.00	27.5	0.51	1.07	3.70	1.59
SC0.1-21-BZ-04	21	54.00	27.7	0.51	1.07	3.70	1.58
SC0.1-21-BZ-05	21	54.00	28.0	0.52	1.10	3.60	1.52
				Average	1.09	Average	1.53
SC0.1-28-BZ-01	28	54.00	27.5	0.51	1.12	3.30	1.42
SC0.1-28-BZ-02	28	54.00	21.7	0.40	1.14	3.50	1.90
SC0.1-28-BZ-03	28	54.00	26.8	0.50	1.07	3.80	1.67
SC0.1-28-BZ-04	28	54.00	26.9	0.50	1.06	3.80	1.67
SC0.1-28-BZ-05	28	54.00	26.4	0.49	1.11	3.70	1.65
				Average	1.10	Average	1.66

Table 4.10 Results of the Brazilian tensile strength testing with Specimen of S:C = 2:10.

Admixture	Curing time	Diameter (mm)	Thick (mm)	L/D	Density (g/cc)	Normal load (KN)	Tensile strength (MPa)
SC0.2-07-BZ-01	7	54.00	28.0	0.52	1.08	3.50	1.47
SC0.2-07-BZ-02	7	54.00	27.7	0.51	1.07	3.50	1.49
SC0.2-07-BZ-03	7	54.00	28.0	0.52	1.06	3.50	1.47
SC0.2-07-BZ-04	7	54.00	27.5	0.51	1.07	3.60	1.54
SC0.207-BZ-05	7	54.00	28.0	0.52	1.09	3.60	1.52
				Average	1.08	Average	1.50
SC0.2-14-BZ-01	14	54.00	28.0	0.52	1.09	3.20	1.35
SC0.2-14-BZ-02	14	54.00	27.7	0.51	1.09	3.80	1.62
SC0.2-14-BZ-03	14	54.00	28.0	0.52	1.09	3.50	1.47
SC0.2-14-BZ-04	14	54.00	27.0	0.50	1.08	3.60	1.57
SC0.2-14-BZ-05	14	54.00	28.0	0.52	1.10	3.60	1.52
				Average	1.09	Average	1.51
SC0.2-21-BZ-01	21	54.00	28.0	0.52	1.11	3.20	1.35
SC0.2-21-BZ-02	21	54.00	27.5	0.51	1.11	3.80	1.63
SC0.2-21-BZ-03	21	54.00	28.0	0.52	1.09	3.50	1.47
SC0.2-21-BZ-04	21	54.00	27.7	0.51	1.11	3.60	1.53
SC0.2-21-BZ-05	21	54.00	28.0	0.52	1.10	4.00	1.69
				Average	1.10	Average	1.53
SC0.2-28-BZ-01	28	54.00	25.8	0.48	1.11	3.20	1.46
SC0.2-28-BZ-02	28	54.00	27.2	0.50	1.11	4.10	1.78
SC0.2-28-BZ-03	28	54.00	26.4	0.49	1.05	3.90	1.74
SC0.2-28-BZ-04	28	54.00	26.4	0.49	1.09	3.50	1.56
SC0.2-28-BZ-05	28	54.00	26.4	0.49	1.11	4.50	2.01
				Average	1.10	Average	1.71

Table 4.11 Results of the Brazilian tensile strength testing with Specimen of S:C = 3:10.

Admixture	Curing time	Diameter (mm)	Thick (mm)	L/D	Density (g/cc)	Normal load (KN)	Tensile strength (MPa)
SC0.3-07-BZ-01	7	54.00	28.0	0.52	1.07	3.80	1.60
SC0.3-07-BZ-02	7	54.00	28.0	0.52	1.08	3.80	1.60
SC0.3-07-BZ-03	7	54.00	28.0	0.52	1.08	4.00	1.69
SC0.3-07-BZ-04	7	54.00	27.5	0.51	1.09	4.30	1.84
SC0.3-07-BZ-05	7	54.00	28.0	0.52	1.11	3.60	1.52
				Average	1.09	Average	1.65
SC0.3-14-BZ-01	14	54.00	27.5	0.51	1.09	4.00	1.72
SC0.3-14-BZ-02	14	54.00	27.5	0.51	1.09	3.80	1.63
SC0.3-14-BZ-03	14	54.00	28.0	0.52	1.08	4.50	1.90
SC0.3-14-BZ-04	14	54.00	27.5	0.51	1.09	4.30	1.84
SC0.3-14-BZ-05	14	54.00	28.0	0.52	1.11	3.60	1.52
				Average	1.09	Average	1.72
SC0.3-21-BZ-01	21	54.00	28.0	0.52	1.11	4.00	1.69
SC0.3-21-BZ-02	21	54.00	28.0	0.52	1.11	3.80	1.60
SC0.3-21-BZ-03	21	54.00	27.8	0.51	1.12	4.50	1.91
SC0.3-21-BZ-04	21	54.00	27.5	0.51	1.06	4.30	1.84
SC0.3-21-BZ-05	21	54.00	28.0	0.52	1.13	3.60	1.52
				Average	1.11	Average	1.71
SC0.3-28-BZ-01	28	54.00	27.7	0.51	1.14	4.00	1.70
SC0.3-28-BZ-02	28	54.00	27.4	0.51	1.11	4.30	1.85
SC0.3-28-BZ-03	28	54.00	27.8	0.51	1.12	4.25	1.80
SC0.3-28-BZ-04	28	54.00	26.4	0.49	1.06	4.20	1.88
SC0.3-28-BZ-05	28	54.00	28.8	0.53	1.13	3.50	1.43
				Average	1.11	Average	1.73

Table 4.12 Results of the Brazilian tensile strength testing with Specimen of S:C = 4:10.

Admixture	Curing time	Diameter (mm)	Thick (mm)	L/D	Density (g/cc)	Normal load (KN)	Tensile strength (MPa)
SC0.4-07-BZ-01	7	54.00	27.7	0.51	1.11	4.40	1.87
SC0.4-07-BZ-02	7	54.00	28.0	0.52	1.05	4.00	1.69
SC0.4-07-BZ-03	7	54.00	27.8	0.51	1.12	3.80	1.61
SC0.4-07-BZ-04	7	54.00	28.0	0.52	1.08	4.20	1.77
SC0.4-07-BZ-05	7	54.00	28.0	0.52	1.09	4.10	1.73
				Average	1.09	Average	1.73
SC0.4-14-BZ-01	14	54.00	27.7	0.51	1.12	4.40	1.87
SC0.4-14-BZ-02	14	54.00	28.0	0.52	1.11	4.00	1.69
SC0.4-14-BZ-03	14	54.00	27.8	0.51	1.11	3.80	1.61
SC0.4-14-BZ-04	14	54.00	27.5	0.51	1.09	4.20	1.80
SC0.4-14-BZ-05	14	54.00	27.5	0.51	1.11	4.30	1.84
				Average	1.11	Average	1.76
SC0.4-21-BZ-01	21	54.00	28.0	0.52	1.09	4.40	1.85
SC0.4-21-BZ-02	21	54.00	27.5	0.51	1.14	4.00	1.72
SC0.4-21-BZ-03	21	54.00	27.8	0.51	1.13	3.80	1.61
SC0.4-21-BZ-04	21	54.00	28.0	0.52	1.07	4.20	1.77
SC0.4-21-BZ-05	21	54.00	28.0	0.52	1.17	4.30	1.81
				Average	1.12	Average	1.75
SC0.4-28-BZ-01	28	54.00	26.9	0.50	1.09	4.50	1.97
SC0.4-28-BZ-02	28	54.00	27.4	0.51	1.14	3.00	1.29
SC0.4-28-BZ-03	28	54.00	27.8	0.51	1.13	4.00	1.70
SC0.4-28-BZ-04	28	54.00	26.4	0.49	1.07	4.70	2.10
SC0.4-28-BZ-05	28	54.00	28.8	0.53	1.17	5.00	2.05
				Average	1.12	Average	1.82

Table 4.13 Results of the Brazilian tensile strength testing with Specimen of S:C = 5:10.

Admixture	Curing time	Diameter (mm)	Thick (mm)	L/D	Density (g/cc)	Normal load (KN)	Tensile strength (MPa)
SC0.5-07-BZ-01	7	54.00	28.0	0.52	1.09	4.20	1.77
SC0.5-07-BZ-02	7	54.00	27.5	0.51	1.12	4.30	1.84
SC0.5-07-BZ-03	7	54.00	28.0	0.52	1.11	4.50	1.90
SC0.5-07-BZ-04	7	54.00	28.0	0.52	1.12	4.00	1.69
SC0.5-07-BZ-05	7	54.00	28.0	0.52	1.11	4.20	1.77
				Average	1.11	Average	1.79
SC0.5-14-BZ-01	14	54.00	28.0	0.52	1.12	4.50	1.90
SC0.5-14-BZ-02	14	54.00	27.5	0.51	1.12	4.00	1.72
SC0.5-14-BZ-03	14	54.00	27.7	0.51	1.12	4.50	1.92
SC0.5-14-BZ-04	14	54.00	28.0	0.52	1.12	3.80	1.60
SC0.5-14-BZ-05	14	54.00	28.0	0.52	1.11	4.20	1.77
				Average	1.12	Average	1.78
SC0.5-21-BZ-01	21	54.00	27.7	0.51	1.14	4.50	1.92
SC0.5-21-BZ-02	21	54.00	28.0	0.52	1.13	4.00	1.69
SC0.5-21-BZ-03	21	54.00	27.5	0.51	1.07	4.50	1.93
SC0.5-21-BZ-04	21	54.00	28.0	0.52	1.16	3.80	1.60
SC0.5-21-BZ-05	21	54.00	27.5	0.51	1.08	4.20	1.80
				Average	1.12	Average	1.79
SC0.5-28-BZ-01	28	54.00	27.7	0.51	1.14	4.50	1.92
SC0.5-28-BZ-02	28	54.00	27.4	0.51	1.13	5.00	2.15
SC0.5-28-BZ-03	28	54.00	26.1	0.48	1.07	4.20	1.90
SC0.5-28-BZ-04	28	54.00	25.6	0.47	1.16	4.00	1.84
SC0.5-28-BZ-05	28	54.00	26.1	0.48	1.08	4.70	2.12
				Average	1.12	Average	1.99

4.3 Push-out Resistance Tests

The objective of this test is to determine the axial mechanical strength of rock salt core plugs in borehole through push-out tests. The curing period for all push-out tests is 7 days. Figure 4.9 shows the push-out test setup. A cylindrical steel rod is applied an axial load to a rock salt core plug. The top displacement of the borehole plug is measured with dial gages. The axial load is measured by a load gage of hydraulic pump. A cylindrical steel plate is centered on the bottom bearing plate of axial bar. The upper horizontal arms supported the top dial gages that measured the top plug displacement. A square platen with a central hole is centered on the circular steel plate with a slit. All of displacement also is measured manually by dial gages with a resolution of 0.025 mm. A loading frame with a hydraulic cylinder applies the load. The machine has a capacity of 50 kN with a resolution of 0.5 kN.

Figure 4.10 shows the push-out test setup. A sludge-mixed cement cylinder in PVC molds with rock salt core is centered on the circular platen. The specimens are loaded under constant stress. The load and top plug displacements are recorded manually at 10 seconds intervals until the sample failed.

The bond strength or the average shear stress (τ_{av}) distribution induced by push-out test loading along the rock salt/cement plug interface can be calculated by the following equation (Stormont and Daeman, 1983):

$$\tau_{av} = F/\pi D_i L \quad (4.2)$$

where F is the failure load, D_i is the plug diameter and L is the rock salt plug length. The dimensions of the sludge-mixed cement cylinder and the bond strength of rock salt core plugs are summarized in Table 4.14.

Figure 4.11 plots the applied axial stress as a function of the top plug displacements. The peak and residual shear stress are plotted against the corresponding S:C ratios. Figure 4.12 shows the post-test after failure in the push-out test. Rock bridges fail at applied axial stresses from 17.77 to 118.01 MPa. The bond strength tends to increase as the sludge-mixed cement ratio (S:C) increase. The highest bond strength is observed from the ratio of S:B = 5:10. Figure 4.13 shows sample which is cut along the axis after failure. The thick rock salt residue on the sludge-mixed cement borehole walls above the (slipped) rock salt core plug and absence of dissolution indicate good bonding.

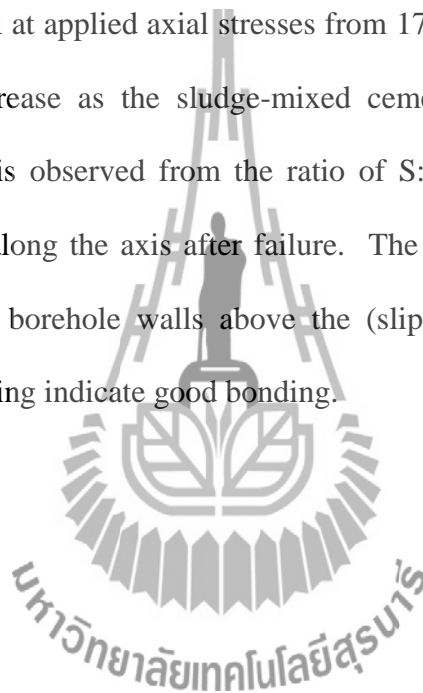


Table 4.14 Dimensions of cement cylinders used for push-out tests, the axial strength (σ_{ax}) and average shear strength (τ_{av}).

Type	Mix ratio	D_o (mm)	L_o (mm)	D_i (mm)	L (mm)	F (kN)	σ_{ax} (MPa)	τ_{av} (MPa)
C	0:10	100.30	101.20	25.40	101.20	9.0	17.77	1.12
S:C	1:10	100.68	101.30	25.40	100.30	24.0	47.39	3.00
S:C	2:10	100.68	101.65	25.30	100.65	25.0	49.75	3.13
S:C	3:10	100.60	101.30	25.40	100.30	40.0	78.98	5.00
S:C	4:10	100.12	101.20	25.60	100.02	46.0	89.41	5.72
S:C	5:10	100.36	101.21	25.45	100.21	60.0	118.01	7.49

D_o = cement cylinder diameter, L_o = cylinder length, D_i = plug diameter, L = rock salt plug length, F = axial load at failure.

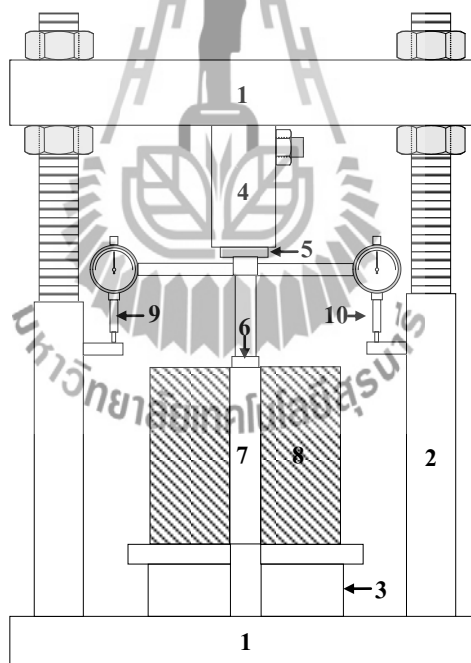


Figure 4.9 Schematic drawing of push-out resistance test setup 1. Loading frame; 2. Vertical steel rods; 3. Steel plate with a slit; 4. Hydraulic cylinder; 5. Loading platen; 6. Axial bar and steel cylinder; 7. Rock salt sample; 8. Sludge-mixed cement sample in PVC mold; 9. and 10. Dial gages.



Figure 4.10 Push-out test setup.

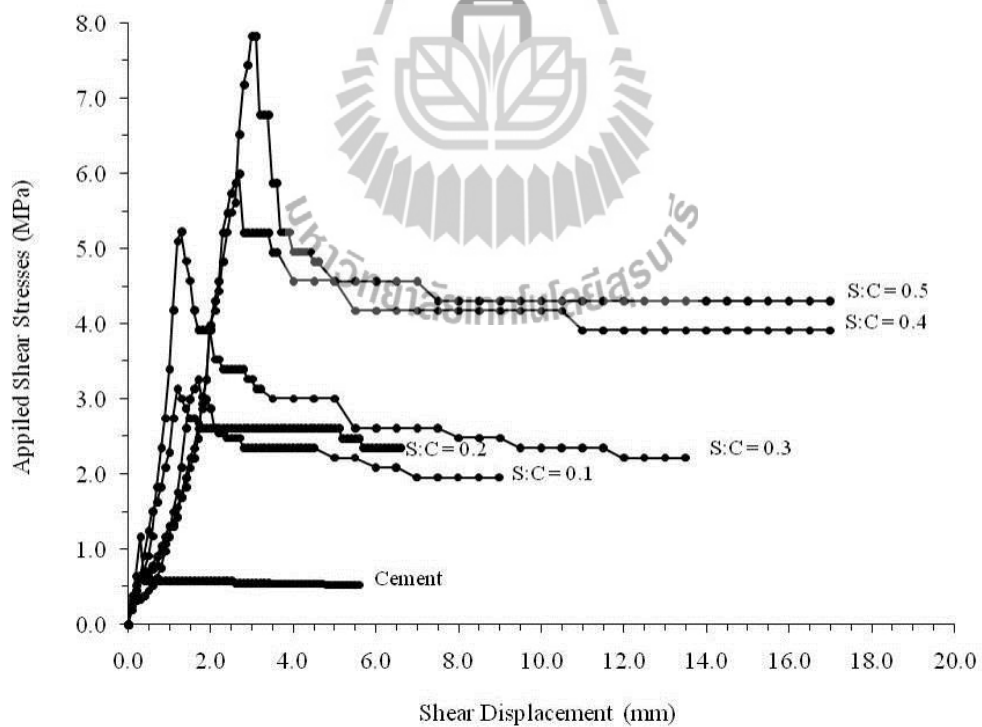


Figure 4.11 Applied shear stress vs. top axial rock salt core displacement for the push-out resistance test.

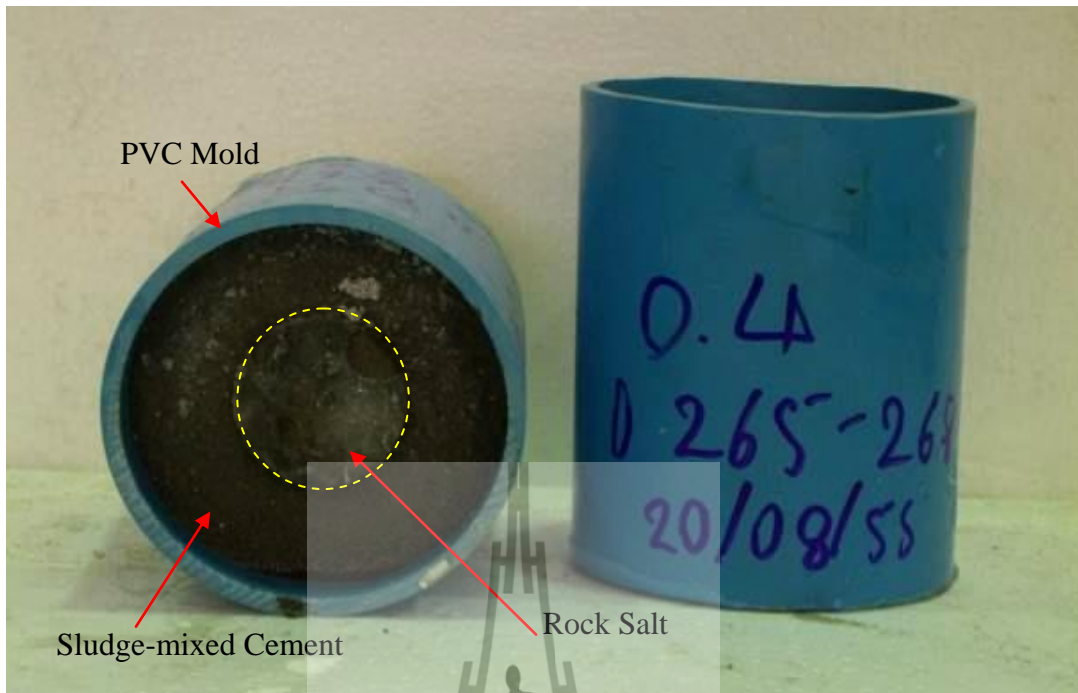


Figure 4.12 Specimen after failure in the push-out test.



Figure 4.13 Specimen after failure in the push-out test.

4.4 Permeability Testing of Grouting Materials

The permeability of grouting materials is determined in terms of the intrinsic permeability (k). The constant head flow test is conducted to measure the longitudinal permeability of the grout. Test pressure and specimen configuration are measured and used to calculate the coefficient of permeability. The permeability of the system considered herein is measured using a constant head apparatus as shown in Figure 4.14. The flow in longitudinal direction of a tested system is described by Darcy's law. The coefficient of permeability, K , can be calculated from the equation. (Indraratna & Ranjith, 2001)

$$K = Q/Ai \quad (4.3)$$

where Q is volume flow rate (m^3/s); A is cross-sectional area of sludge-mixed cement grout (m^2); and i is the hydraulic gradient. The intrinsic permeability (k) can be determined from the equation.

$$k = K\mu/\gamma_w \quad (4.4)$$

where K is the coefficient of permeability (m/s); μ is dynamic viscosity of saturated brine and γ_w is density of liquid water from 20 degree Celsius ($9,789 \text{ N/m}^3$). The cylinder specimen is 10 cm in diameter and 10 cm long. The permeability of the test system is measured and recorded at 7, 14, 21 and 28 days of curing periods. The results indicate that when the curing time increases the intrinsic permeability (k) of cement grout decreases. The conductivity of permeability and intrinsic permeability of sludge-

mixed cement grouts as a function of curing time and shown in Figure 4.15 and 4.16, respectively.

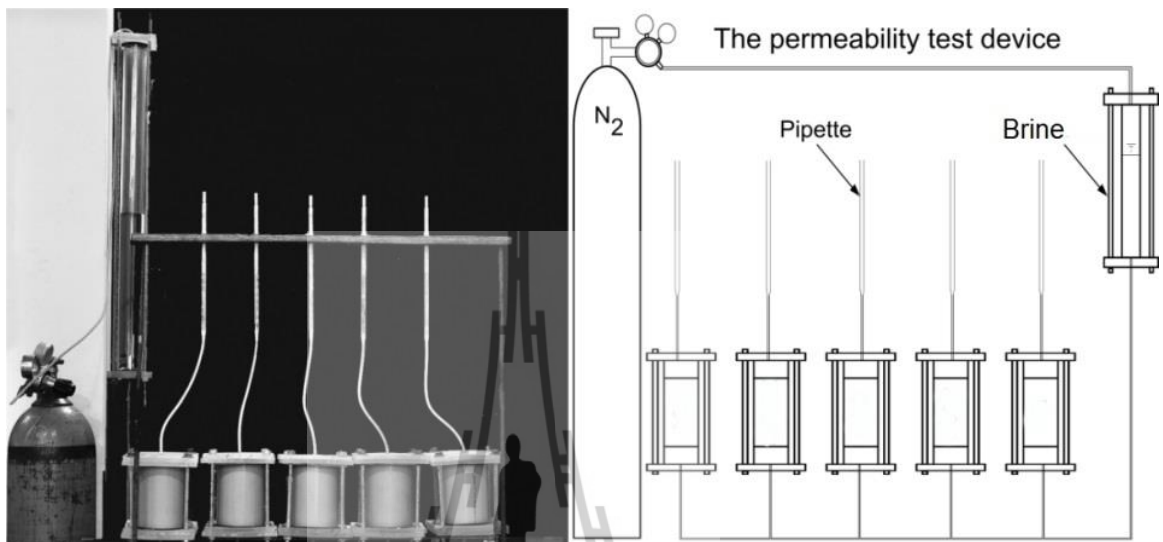


Figure 4.14. Constant head flow test apparatus used for permeability testing of grouting materials.

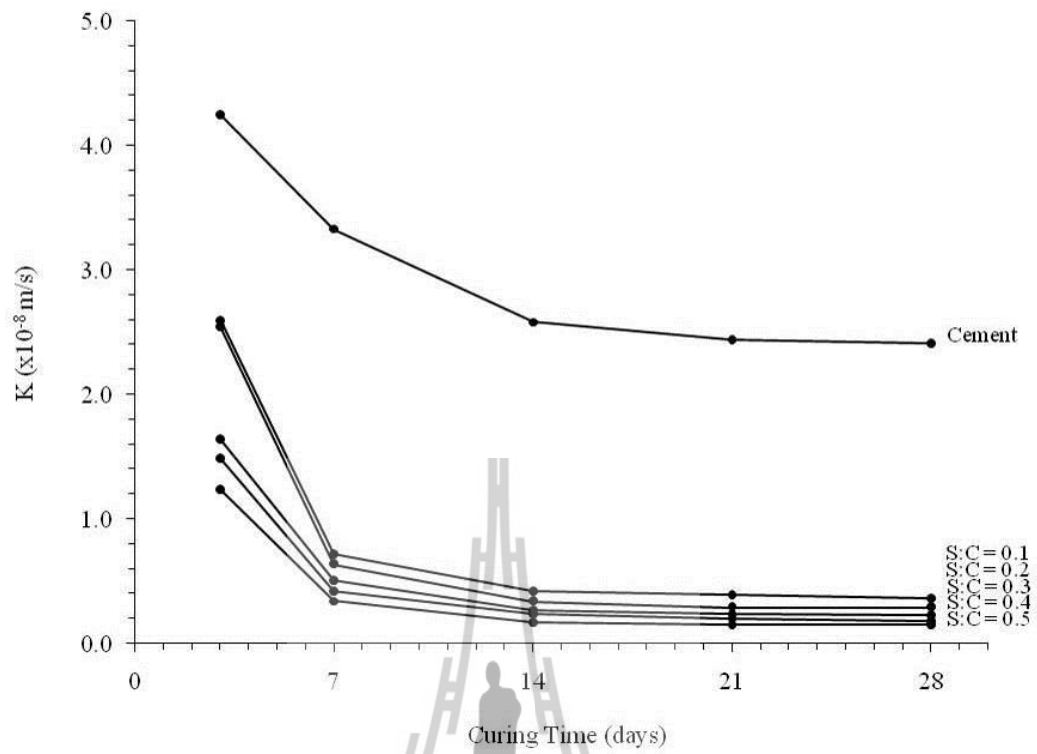


Figure 4.15 Conductivity of permeability of sludge-mixed cement as a function of time.

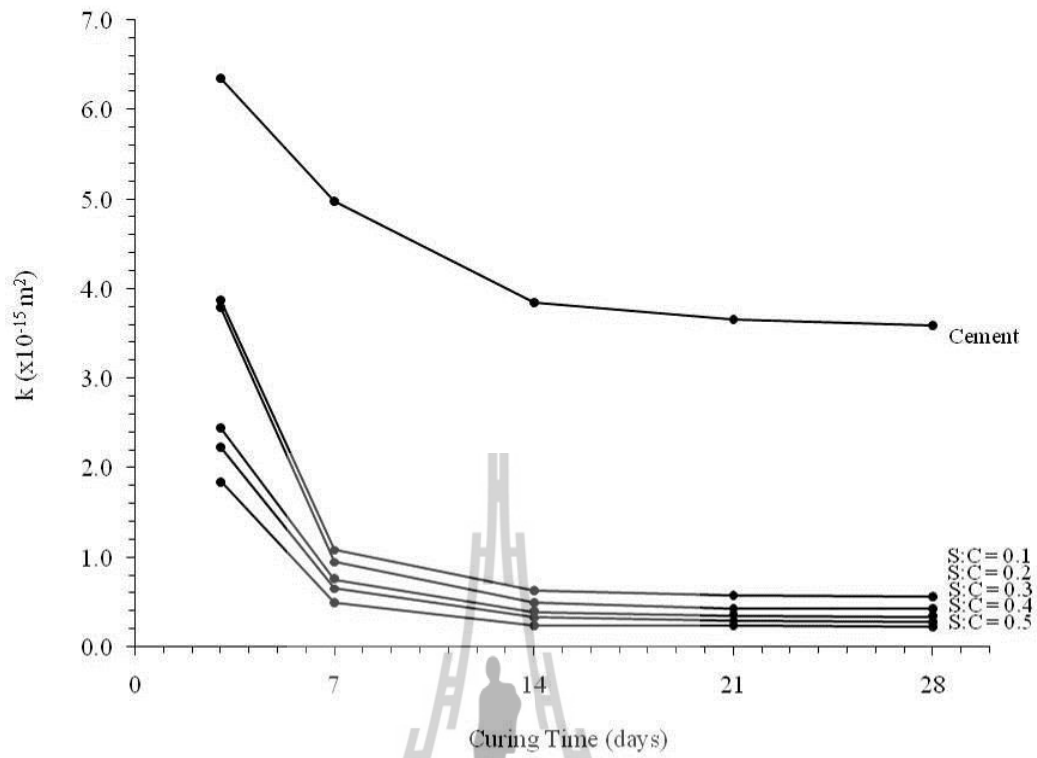


Figure 4.16. Intrinsic permeability of sludge-mixed cement as a function of time.

CHAPTER V

DISCUSSIONS, CONCLUSIONS, AND RECOMMENDATIONS FOR FUTURE STUDIES

5.1 Discussions and conclusions

The sludge-mixed cement grouts are prepared from the commercial grade Portland cement mixed with Bang Khen water treatment sludge, saturated brine and chloride resistant agent have been tested to determine the mechanical and hydraulic performance. This study aims to determine the appropriate slurry viscosity and strength of the sludge-mixed cement grouting. The results lead to the selection of the most suitable ratio of sludge-mixed cement (S:C) for grouting in rock salt fractures.

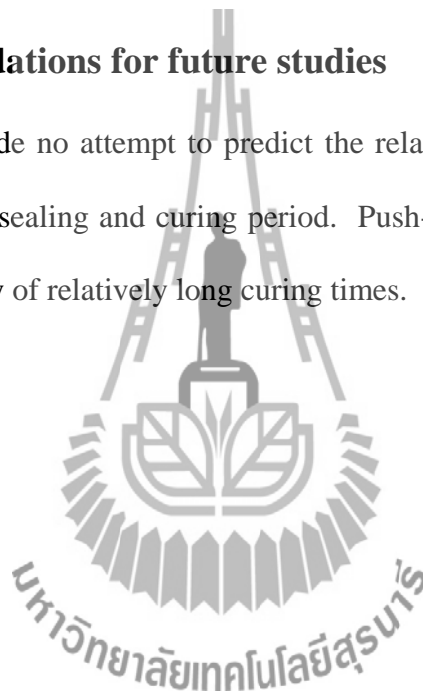
Six rock salt cores are plugged within cement cylinder for push-out tests. Average interface shear strengths range from 1.12 to 7.49 MPa with a various of S:C ratio (assuming uniform shear stress distributions). Samples showing high axial strength generally lead to high bond strength. The bottom plug displacements are smaller compared to the top axial displacements prior to bond failure. Upon plug slip, the difference between the top and bottom plug displacements mostly decrease most probably due to stress relief caused by slip along the interface. The Brazilian tensile strength indicate that the bond strength between the cured sludge-mixed cement grout and rock salt fractures varies from 1.34 to 1.82 MPa with a various of S:C ratio.

The permeability of the sludge-mixed cement grouting materials measured from the longitudinal flow test with constant head decreases with curing time at 7, 14,

21 and 28 days. The results indicate that when the curing time increases the intrinsic permeability (k) of cement grout decreases. The mixture with the S:C of 5:10 by weight gives the lowest permeability. The S:C mixtures have the mechanical and hydraulic properties equivalent to those of the commercial grade Portland cement mixtures which indicates that the sludge can be used as a substituted material to mix with cement for salt fracture grouting purpose.

5.2 Recommendations for future studies

This study made no attempt to predict the relation between bond strength of sludge-mixed cement sealing and curing period. Push-out tests should be performed on plugs with a variety of relatively long curing times.



REFERENCES

- Butron, C., Gustafson, G., Fransson, A., and Funehag, J. (2010). Drip sealing of tunnels in hard rock: A new concept for the design and evaluation of permeation grouting. **Tunnelling and Underground Space Technology**. 25: 114-121.
- Detoumay, E. (1980). Hydraulic Conductivity of Closed Rock Fractures: An Experimental and Analytical Study. **Proceeding of the 13th Canadian Rock Mechanics Symposium** (pp 168-173). Toronto: (n.p.).
- Gangi, A. F. (1978). Variation of Whole and Fractured Porous Rocks Permeability with Confining Pressure. **International Journal of Rock Mechanics and Mining Sciences & Geomechanics Abstracts**. 15: 249-257.
- Hadsanan, P., Lertpocasombut, K. and Chatveera, B. (2006). Mechanical properties and durability of cement mortar containing dry sludge ash from Bang Khen water supply plant. **National Convention on Civil Engineering 2006 (NCCE11)**, 20-22 April 2006, Phuket.
- Indraratna, B., and Ranjith, P. (2001). **Hydromechanical Aspects and Unsaturated Flow in Joints Rock**. Lisse: A. A. Balkema.
- Japakasetr, T. (1992). Thailand's mineral potential and investment opportunity, **National Conference on Geologic Resources of Thailand: Potential for Future Development**, November 1992, DMR, Bangkok, Thailand, pp. 641-652.
- Japakasetr, T. (1985). Review on rock salt and potash exploration in Northeast Thailand, **Conference on Geology and Mineral Resources Development of**

- the Northeast, Thailand, 26-29 November 1985**, Thailand: Khon Kaen University, pp. 135-147.
- Japakasetr, T. and Workman, D. R. (1981). Evaporite deposits of northeast Thailand, **Circum-Pacific Conferences**, Hawaii, pp. 179-187.
- Jones, F. O. (1975). A Laboratory Study of the Effects of Confining Pressure on Fracture Flow and Storage Capacity in Carbonate Rocks. **Journal of Petroleum Technology**. 21: 21-27.
- Kashir, M., and Yanful, E. K. (2000). Compatibility of Slurry Wall Backfill Soils With Acid Mine Drainage. **Advances in Environmental Research** 4 : 251-268.
- Nelson, R. (1975). **Fracture Permeability in Porous Reservoirs**: Experimental and Field Approach. Ph.D. dissertation, Department of Geology, Texas A&M University.
- Owaidat, L. M., Andromalos, K. B., and Sisley, J. L. (1999). Construction of a Soil-Cement-Bentonite Slurry Wall for a Levee Strengthening Program. **Association of State Dam Safety Officials Annual Conference**, 10-12 October 1999, St. Louis, Missouri.
- Rahmani, H. (2004). Estimation of grout distribution in a fractured rock by numerical modeling. **A thesis submitted in partial fulfilment of the requirements for the degree of master of applied science in the faculty of graduate studies (Civil Engineering)**, University of Tehran.
- Rattanajarurak, P. (1990). **Formation of The Potash Deposits, Khorat Plateau, Thailand**. M.S. Thesis, School of Mine, Kensington, Australia.
- Sattayarak, N. (1983). Continental Mesozoic stratigraphy of Thailand, **Symposium on Stratigraphy of Thailand**, 18-19 November, Bangkok, pp. 77-80.

- Sattayarak, N. (1983). Review of continental Mesozoic stratigraphy of Thailand: **Proceeding Stratigraphic correlation of Thailand and Malaysia**, Geol. Soc. Thailand, Vol. 1 : 127-148.
- Sattayarak, N. (1985). Review on Geology of Khorat plateau, **Conference on Geology and Mineral Resources Development of the Northeast, Thailand 26-29 November 1985**, Thailand: Khon Kaen University, pp. 23-30.
- Snow, D. T. (1968). Anisotropic Permeability of Fractured Media. **Water Resources Research**. 5(6): 1273-1289.
- Suriyachat, D., Vichitamornpun, P. and Ruengsumrej, W. (2004). Water treatment sludge utilization. **Technical Report No. 16/2547. department of primary industries and mines**, Bangkok.
- Sattayarak, N. and Polachan, S. (1990). Rock salt beneath the Khorat plateau (in Thai), In **Proceedings of the Conference on Geology and Mineral Resources of Thailand** (pp. 1-14). Bangkok, Thailand: Department of Mineral Resources.
- Suwanich, P. (1986). **Potash and Rock Salt in Thailand : Nonmetallic Minerals Bulletin No.2**, Economic Geology Division, Department of Mineral Resources, Bangkok, Thailand.
- Sattayarak, N. (1985). Review on Geology of Khorat plateau, **Conference on Geology and Mineral Resources Development of the Northeast, Thailand 26-29 November 1985**, Thailand: Khon Kaen University, pp. 23-30.
- Utha-aroon, C. (1993). Continental origin of the Maha Sarakham evaporites, Northeastern Thailand, **Journal of Southeast Asian Earth Sciences**, 1993, Great Britain, Vol. 8(1-4) : 193-203.

- Valls, S., Yague, A., Vazquez, E. and Mariscal, C. (2004) Physical and mechanical properties of concrete with added dry sludge from a sewage treatment plant. **Cement and concrete research**, 34 : 2203 - 2208.
- Wetchasat and Fuenkajorn, (2012) Laboratory assessment of mechanical and hydraulic performance of sludge-mixed cement grout in rock fractures, **Proceedings of the third Thailand symposium on rock mechanics** : pp 143 - 152.
- Warren, J. (1999). **Evaporites: Their Evolution and Economics**, Blackwell Science, 438pp.
- Yumuang, S. (1983). **On the origin of evaporite deposits in the maha sarakham formation in Bamnet Narong area, Changwat Chaiyaphum**, M.S. thesis, Chulalongkorn University, Thailand.
- Yumuang, S., Khantapab, C., and Taiyagupt, M. (1986). The evaporate deposits in Bamnet Narong area, Northeastern Thailand, **Proceedings of the GEOSEA V** (Bullrtin 20, Vol. 2, pp. 249-267). Geological Society of Malasia.

BIOGRAPHY

Mr. Phadet Deethouw was born on July 6, 1985 in Surin province, Thailand. He received his Bachelor's Degree in Engineering (Geotechnology) from Suranaree University of Technology in 2004. For his post-graduate in 2010, he continued to study with a Master's degree in the Geological Engineering Program, Institute of Engineering, Suranaree university of Technology. During graduation, 2010-2013, he was a full time worker in position of Geotechnical Engineer, Company of Instrument Engineering, Geotechnical and Foundation Engineering (GFE).

